学位論文

The regulatory mechanism of photosynthetic electron transport in higher plants

高等植物における光合成電子伝達の調節メカニズムに関する研究

平成 16 年 12 月博士（生命科学）申請

東京大学大学院新領域創成科学研究科

先端生命科学専攻

樋口　美栄子

TABLE OF CONTENTS

ACKNOWLEDGEMENTS

I would first like to express my sincere gratitude to Prof. Kintake Sonoike for his support throughout my doctor course. I could not accomplish my research without his help. His critical advices are sometimes severe for me but he always provided me valuable insight that I was able to resolve the problem. I will keep his comment in my mind throughout my future work.

I am very grateful to Prof. Yoshikazu Ohya for his precise advices. His comment was always appropriate and caught the essence of the problem. I want to emulate his excellence in my future research life.

I would extend my thanks to Hideki Kudo, Hiroshi Ozaki, Tamaki Fujimori, Mari Kurosawa, Hanayo Sato and Hiroyuki Usuki for their experimental advices and valuable suggestions. They always supported me as members of photosynthesis group. I appreciate very much the helpful advices of Fumi Sano, Masashi Yukawa, Satoru Nogami and Satoru Ishihara. I have learned so much in professional attitude, which made the research successful. I am grateful to Daisuke Watanabe, Yuri Nagai, Ayaka Saka, and Masaya Suzuki for their hearty encouragement. I have received great support and encouragement from Keiko Kono, Tomoyuki Fukuda, and Genjiro Suzuki. They gave me the necessary time to relax from the work. I want to thank members of signal transduction for their encouragement. They gave me a pleasing ambience in the laboratory. I also wish to thank my family for financial support during my doctor course.

LIST OF FIGURES

LIST OF TABLES

ABBREVIATIONS

bp : base pair

kDa : kilodalton

PCR : polymerase chain reaction

P700 : the primary electron donor of photosystem I

Rubisco : ribulose-1,5-bisphosphatase carboxylase/oxygenase

Fd : ferredoxin

PQ : plastoquinone

NADPH : nicotinamide adenine dinucleotide phosphate

ATP : adenosine triphosphate

VDE : violaxanthin de-epoxidase

NPQ : non-photochemical quenchings

PS : photosystem

ABSTRACT

In order to investigate molecular mechanisms of alternative electron pathways in photosynthesis, I screened Arabidopsis mutants using chlorophyll fluorescence that reflects electron transport in photosynthesis. From 16,000 seedlings, I isolated four mutants (36-2-20, 38-14-15, 22-18-21, 37-19-7) having slight modification in the kinetics of chlorophyll fluorescence. The 37-19-7 mutant carried an amino acid substitution in *pgr5* gene that is involved in FQR-mediated cyclic electron flow around PSI. The 22-18-21 mutant was impaired in NDH-dependent cyclic electron flow around PSI. The differences in the phenotype between the two mutants revealed that FQR and NDH-dependent pathways might function distinctly in response to the redox state of the PQ pool. In 36-2-20 mutant, T-DNA was inserted in *hma1* gene encoding a $P1_B$-type ATPase. The *hma1* showed a pale green phenotype in the presence of excess Zn and its defect was rescued by the addition of Fe. Chlorophyll fluorescence analysis suggested that PSI-dependent cyclic electron flow was impaired in *hma1*. These results indicate that HMA1 is involved in Zn transport and Fe deficiency caused by excess Zn might lead to the alteration of the cyclic electron flow around PSI. Chlorophyll fluorescence analysis under various air conditions suggested that the 38-14-15 mutant had defect in photorespiration. Under high light condition, low wave phenomenon, which is a symptom of enhanced cyclic electron flow, was observed in the 38-14-15 mutant. The result suggests that the inhibition of photorespiration may lead to the enhancement of cyclic electron flow around PSI.

INTRODUCTION

Light is critical for the growth and development of photosynthetic organisms. In the reaction of photosynthesis, light energy is transformed to chemical energy through electron transport, resulting in the formation of ATP and NADPH necessary for carbon fixation. However, too much light is known to lead to photooxidative damage (Aro et al. 1993). Under high light condition, limited availability of electron acceptors, especially of CO_2, results in the excess reduction of photosynthetic electron transport chain. Over-reduction of electron carriers may increase the rate of production of the reactive oxygen species. To avoid such condition, most plants have developed the ability to adjust themselves in response to the changes in the light condition.

Changes in the level of irradiance may elicit responses at the level of chloroplasts. Responses of this level can be divided into two categories based on the time scale of the response; long-term responses (acclimation) and short-term responses. Acclimation responses require as long as several days to complete and accompany the change in gene expressions. Acclimation processes include increase in the capacity for CO_2 fixation and photosynthetic electron transport (Andersson et al. 1995), recruitment of enzymes with an anti-oxidant function such as superoxide dismutase (Smirnoff 2000), adjustment of photosystem stoichiometry (Chow et al. 1990) and decrease in the size of the light-harvesting antennae that are associated with photosystems (Bailey et al. 2001).

Short-term responses take place on a timescale of seconds to minutes. Plants that are exposed to rapidly changing light condition need to respond quickly to prevent

photodamage. As one of such responses, chloroplasts possess a photoprotective mechanism to safely dissipate excessive light energy as harmless heat energy. This process, which can be estimated as non-photochemical quenching (NPQ) of chlorophyll fluorescence, is observed in almost all photosynthetic eukaryotes (Baroli, 2000, Muller et al. 2001, Niyogi, 1999). This energy dissipation in NPQ is conducted through the inter-conversion of xanthophyll pigments; violaxanthin, antheraxanthin and zeaxanthin (Yamamoto et al. 1962). Under limiting light condition, zeaxanthin epoxidase converts zeaxanthin to violaxanthin via the intermediate antheraxanthin. In excessive light, violaxanthin is rapidly converted via antheraxanthin to zeaxanthin by the action of the enzyme violaxanthin de-epoxidase (VDE). These cyclic conversions of zeaxanthin, antheraxanthin and violaxanthin are called xanthophyll cycle. An additional factor, PsbS subunit of photosystem (PS) II, has been shown to be involved in NPQ (Li et al. 2000). The acidification of thylakoid lumen due to photosynthetic electron transport is also necessary for the induction of NPQ (Demmig-Adams 1990). Lumenal acidification activates VDE and causes the protonation of PsbS and possibly of other PSII proteins. This protonation is thought to cause some conformational change in PsbS that is necessary for the formation of NPQ. A number of mutants that has defect in xanthophyll cycle activity have been isolated and characterized in detail. For example, the Arabidopsis mutant, *pgr1,* lacks the ability of lumen acidification of the thylakoid membranes leading to a defect in thermal dissipation, which was observed as low levels of NPQ (Munekage et al. 2002).

Thus, the electron flow is a prerequisite for the formation of NPQ. In

oxygenic photosynthesis, PSII and PSI cooperate to achieve a linear electron flow from H_2O to $NADP^+$ and to generate a trans-membrane proton gradient driving ATP synthesis. ATP can also be produced by PSI alone through cyclic electron transfer (Huber and Edwards 1976). There are at least two pathways in cyclic electron transport around PSI (Joliot and Joliot, 2002). One of the pathways is thought to occur via Ferredoxin-quinone oxidoreductase (FQR). Other pathway is catalyzed by NADPH plastoquinone oxidoreductase (NDH) that is homologous to complex I of mitochondria. Although the existence of cyclic electron transport was discovered nearly 50 years ago, it has been a matter of debate whether this electron flow around PSI has physiological relevance in photosynthesis. Recently, Munekage et al. (2002) isolated an Arabidopsis *pgr5* mutant that have defect in cyclic electron flow around PSI using chlorophyll fluorescence imaging system. The *pgr5* mutant could not induce NPQ due to insufficient ΔpH formation. Furthermore, they demonstrated that cyclic electron flow around PSI is essential for PSI photoprotection. On the other hand, the Arabidopsis *crr2* mutant is shown to be impaired in NDH activity due to the lack of RNA processing of *ndhB* gene (Hashimoto et al. 2003). The *crr2 pgr5* double mutant exhibited severe defect in photosynthetic electron transport, indicating that cyclic electron flow around PSI is essential for photosynthesis (Munekage et al. 2004). So far, PGR5 is the only factor reported to be involved in FQR pathway of cyclic electron flow around PSI. The comprehensive vision of cyclic electron flow around PSI is not available at present.

In addition to the cyclic electron transport around PSI, it is suggested that reduction of oxygen by PSI might contribute to ΔpH formation. In this case, electron

transfer to oxygen results in the generation of O_2^-, which can be converted to H_2O_2 by spontaneous dismutation or by the action of superoxide dismutase. Ascorbate is used for the conversion of H_2O_2 to H_2O by the enzymatic reaction catalyzed by ascorbate peroxidase. The oxidized ascorbate, monodehydroascorbate radical, can be re-reduced by electrons from PSI. These reactions are termed the water-water cycle because electrons generated from the oxidation of water at PSII are used for the reduction of O_2 to produce water at PSI (Asada 2000, Heber et al. 2001). It has been implied that the photoreduction of oxygen to water accounts for substantial part of electron transport up to 30%, but no direct evidence has been provided.

Oxygen also plays important roles in photorespiration process. Photorespiration results from the oxygenase reaction catalyzed by Rubisco in chloroplasts, but also involves many reactions in mitochondria and peroxisomes (Wingler, 2000, Douce and Neuburger, 1999). The ratio of the carboxylation rate to the oxygenation rate of Rubisco is dependent on the CO_2 and O_2 concentrations (Farquhr et al. 1980). Under ambient atmospheric conditions, about 20% of the total electron flux through Rubisco is diverted to oxygen. To elucidate the mechanism of photorespiration, several mutants have been isolated in Arabidopsis (Somerville and Ogren 1979, 1980, 1981,1982) and barley (Murray et al. 1987, 1989, Blackwell et al. 1990). These mutants are lethal in normal air condition, but the growth of these mutants is indistinguishable from WT under high CO_2 condition in which photorespiration is suppressed. During the photorespiration process, CO_2 and NH_3 are released and ATP and NADPH are consumed. Photorespiration seems to be a wasteful reaction but it was reported that

photorespiration could serve as an electron sink to prevent over-reduction of photosynthetic electron transport, especially under stress condition.

As described above, alternative electron pathways such as cyclic electron transport around PSI, water-water-cycle and photorespiration are thought to serve as electron sink to prevent photodamage when CO_2 fixation is limited under some stress conditions. However, only a few mutants defective in alternative electron pathway have been isolated and exact physiological role of those reactions are poorly defined at present. For the better understanding of the alternative electron transport as a regulatory mechanism in photosynthesis, here I report the isolation of mutants that are defective in alternative electron transport. Through the characterization of those isolated mutants, information on the alternative electron transport under different environmental conditions were obtained.

MATERIALS AND METHODS

Plant material and Growth condition

Seeds of *Arabidopsis thaliana* cv Ws-2 (Wassilewskija) and T-DNA transformed populations were provided by the Arabidopsis Biological Resource Center (The Ohio State University). Arabidopsis plants were grown in Murashige and Skoog (MS) agar plates supplemented with sucrose (1%, w/v) or in soil. Plants were grown at 23^{o}C under continuous illumination (80 μmol photons m^{-2} s^{-1}).

Chlorophyll fluorescence screening

For screening, plants were grown in plates for 7-8 days. Chlorophyll fluorescence kinetics was monitored during illumination (350 μmol photons m^{-2} s^{-1}) after pre-illumination for 40 sec (350 μmol photons m^{-2} s^{-1}) and subsequent dark-adaptation for 1 min using chlorophyll fluorescence monitoring system (Fluorcam, Photon Systems Instruments, Czech).

Chlorophyll fluorescence measurement

Chlorophyll fluorescence parameters were determined using a pulse-modulated fluorometer (PAM 101/103; Walz, Effeltrich, Germany) as described in Schreiber et al (1993). Minimum fluorescence (Fo) was recorded after dark adaptation at least for 30 min. Maximum fluorescence (Fm) was obtained by applying a 0.8 s saturating light pulse (3,000 μmol photons m^{-2} s^{-1}) from a light source (KL 1500; Schott, Wiesbaden,

Germany). Actinic light was also supplied by KL1500 lamp at indicated photon flux densities. The maximum quantum yield of PSII (Fv/Fm) was calculated as (Fm-F_0)/Fm. The steady state of quantum yield of PSII (Fv'/Fm') was calculated as (Fm'-F_0')/Fm'. The relative rate of electron transport through PSII (ETR) was calculated as (Fm'-F/Fm')×photon flux density. NPQ was calculated as (Fm-Fm')/Fm'. Reduction level of QA (1-qP) was calculated as (Fs-F_0')/(Fm'-F_0'). The partial pressures of CO_2 were controlled with an IRGA system (Li-6400; Licor, Lincoln, NE, USA).

Measurement of the redox change in P700

The redox state of P700 was monitored by absorbance changes at 820 nm using a pulse-modulated system (PAM 101/102; Walz). P700 was oxidized by far-red light from a photodiode (FR-102; Walz). The maximum contents of $P700^+$ (ΔAmax) were estimated by a saturating pulse of multi turnover flash (50 ms) under a far-red light background. ΔA was determined at indicated photon flux densities. The redox state of P700 was calculated as ΔA/ΔAmax

Measurement of NDH activity

Chlorophyll fluorescence was monitored using a pulse amplified modulation chlorophyll fluorometer. Detached leaves were illuminated with actinic light of 200 μmol photons m^{-2} s^{-1} for 2 min before switching off the actinic light. Prior to measurements, leaves were dark-adapted at least for 30 min.

TAIL-PCR method

The region flanking T-DNA insertions was amplified by thermal asymmetric interlaced (TAIL) PCR essentially according to Liu et al. (1995), using degenerate primer DG2 (5'-GT G/A/T/C CGA G/C A/T CA G/A/T/C A A/T GTT-3') in combination with T-DNA left border-specific primers TL-3 (5'-TCT GGG AAT GGC GTA ACA AAG GC-3'), TL-2 (5'-AAC TGT AAT GAC TCC GCG CAA TA-3') and TL-1 (5'-TCT GGG AAT GGC GTA ACA AAG GC-3'). The first PCR program was as follows: 20 cycles of 1 min at 94 °C, 1 min at 50°C and 3 min at 72 °C. The second PCR program was follows: 12 cycles of 30 sec at 94 °C, 1 min at 64 °C, 3 min at 72 °C, 30 sec at 94 °C, 1 min at 64 °C, 3 min at 72 °C, 30 sec at 94 °C, 1 min at 44 °C and 3 min at 72 °C. The third PCR program was follows: 12 cycles of 30 sec at 94 °C, 1 min at 64 °C, 3 min at 72 °C, 30 sec at 94 °C, 1 min at 64 °C, 3 min at 72 °C, 30 sec at 94 °C, 1 min at 50 °C and 3 min at 72 °C. TAIL-PCR products were sequenced using a dye terminator cycle sequencing kit (Applied Biosystems, Tokyo, Japan) and an ABI prism sequencer (ABI PRISM 310, Applied Biosystems, Tokyo, Japan).

Map-based cloning

The mutated genes of the 37-19-7, 22-18-21 and 38-14-15 mutants were mapped with molecular markers based on a cleaved amplified polymorphic sequence (CAPS) (Konieczny and Ausubel, 1993) and simple sequence length polymorphism (SSLP) (Bell and Ecker, 1994). Genomic DNA was isolated from F_2 plants derived from the cross between mutants (genetic background of Wassilewskija) and the Wild type

(Columbia and Landsberg erecta). The CAPS markers are publicly available at The Arabidopsis Information Resource (TAIR) site (http://www.arabidopsis.org). Since polymorphism between Columbia and Landsberg was available at TAIR site, I made several CAPS and SSLP markers. CAPS and SSLP marker used in this study was listed in Table 1. Genomic DNA containing WT and 37-19-7 was amplified by PCR using pgr5 gene specific primers 5'-CAT GAG AAA CGT AAT AAT AAG TTA AGT C–3' and 5'-TCA GCT AAG ACC TTA TTG AAC AAC-3' PCR products were sequenced using a dye terminator cycle sequencing kit and an ABI prism sequencer.

RESULTS

Chlorophyll fluorescence screening

For screening, Arabidopsis plants were grown under low light (80 μmol photons m^{-2} s^{-1}) for 7-8 days. Chlorophyll fluorescence was measured during actinic light illumination (350 μmol photons m^{-2} s^{-1}, 12 sec) using a fluorescence imaging system. Dark-adapted leaves showed characteristic changes in chlorophyll fluorescence as shown in Figure 1. I screened 16,000 Arabidopsis seedlings and isolated four mutants (37-19-7, 22-18-21, 36-2-20, 38-14-15) showing different fluorescence kinetics from WT. Pulse amplitude modulation (PAM) fluorescence system enables us to obtain more precise interpretation of chlorophyll fluorescence signals. In order to characterize isolated mutants, I determined photosynthetic parameters by PAM fluorescence analysis. Photosynthetic parameters were determined at a high photon flux density (700 μmol photons m^{-2} s^{-1}). Table 2 shows the steady-state photosynthetic parameters (Fv/Fm, 1-qP, NPQ, Fv'/Fm' and ETR) of WT and isolated mutants. The Fv/Fm is the maximum quantum yield of PSII. The 1-qP reflects the reduction level of Q_A, a primary quinone acceptor of PSII. The NPQ reflects the non-radiative dissipation of excitation energy. The Fv'/Fm' is the effective quantum yield of PSII in the steady state. The ETR is photosynthetic electron transport rate through PSII. These parameters were used for the characterization of each mutant in the following experiments.

1. The 37-19-7 mutant

Non-photochemical quenching is affected due to insufficient electron flow from PSI

Figure 2 shows the photon flux density dependence of NPQ in WT and the 37-19-7 mutant. NPQ of the 37-19-7 mutant was smaller than that of WT especially under high light condition. Increase in NPQ under high light observed in WT was totally diminished in the 37-19-7 mutant. Since the induction of NPQ requires a low thylakoid lumen pH that is generated by photosynthetic electron transport, electron transport in the 37-19-7 mutant would be impaired under high light condition. Chlorophyll fluorescence mainly reflects the electron transfer at PSII, since the yield of chlorophyll fluorescence of PSI complexes is low at room temperature. To obtain more direct information on the downstream of the electron transfer after PSII, the redox state of P700, the reaction center chlorophyll of PSI, was compared between WT and the 37-19-7 mutant. Figure 3 shows the photon flux density dependence of the redox state of P700 (Figure 3). In WT, P700 was oxidized with increasing photon flux density due to the down-regulation of PSII caused by NPQ. At lower photon flux density, P700 was not so affected in the 37-19-7 mutant, indicating that electron transport was not impaired under normal light condition. On the other hand, the P700 was more reduced in the mutant than in WT at higher photon flux densities, suggesting that electron transport downstream of PSI was inhibited under high-light condition. Thus, the low level of NPQ in the 37-19-7 mutant is possibly caused by insufficient generation of ΔpH due to limited electron transfer downstream of PSI under high-light condition.

The 37-19-7 has a mutation in pgr5 gene

Arabidopsis mutants in this study are generated by T-DNA random insertion mutagenesis with a ecotype Wassilewskija (Ws). T-DNA is a segment of the tumor-inducing (Ti) plasmid of *Agrobacterium tumefaciens* and Arabidopsis mutants contain kanamycin resistance cassette for selection. The 37-19-7 mutant could not grow in the presence of kanamycin, indicating that the observed phenotype could not be ascribed to the insertion of the T-DNA. Therefore, to identify the gene responsible for the phenotype, a mapping population was generated, which consisted of F_2 individuals derived from backcrosses to a wild type plant of different ecotypes (Landsberg and Columbia). For linkage analysis, I used the Cleaved Amplified Polymorphic Sequences (CAPS) and simple sequence length polymorphism (SSLP) method. One CAPS marker in chromosome 2 showed quite lower recombination frequency than other chromosome markers, indicating that the 37-19-7 mutation was mapped to chromosome 2. Further mapping analysis indicated that the mutation of 37-19-7 was closely linked to molecular marker RGA in chromosome 2. Sequencing of the genes with chloroplast transit signals near RGA revealed that the 37-19-7 mutant carried one nucleotide substitution in *pgr5* gene (At2g05620), which lead to an amino acid substitution from Asp125 to Lys (Figure 4). PGR5 is previously shown to be involved in FQR-mediated cyclic electron flow around PSI (Munekage et al. 2002). The screening strategy applied in this study seems to be valid for isolating mutants that have defects in alternative electron pathway, judging from the fact that I could isolate *pgr5* mutant by monitoring the kinetics of chlorophyll fluorescence intensity.

2. The 22-18-21 mutant

NPQ could not be kept high in the 22-18-21 mutant

In the 22-18-21 mutant, steady state NPQ decreased compared to that in WT under high light condition (Table 2). Figure 5 shows the photon flux density dependence of NPQ. NPQ is lower in the 22-18-21 mutant under high light condition although the difference is much smaller at lower photon flux density. Induction and relaxation kinetics of NPQ was shown in Figure 6. In WT, maximum NPQ was attained within 3 min after the onset of actinic light and the level of NPQ was kept high during the illumination. The NPQ relaxed in 5 min after the cessation of the illumination. On the other hand, the 22-18-21 mutant could not maintain maximum NPQ though the early induction of NPQ was essentially the same as that of WT. The low level of NPQ in the 22-18-21 mutant might be also caused by insufficient generation of ΔpH due to decreased electron transfer, similar to the case of the 37-19-7 mutant. However, redox state of P700 of the 22-18-21 mutant did not show significant difference from that of WT (Figure 7).

The redox state of stroma in chloroplast is altered in the 22-18-21mutant

By repetitively illuminating dark-adapted leaves for 30 sec with far-red light, oxidation and reduction kinetics of P700 was observed (Figure 8). In WT, P700 was rapidly oxidized within one second and then the rate of oxidation became slower and reached a plateau (Figure 8A). Oxidation kinetics of P700 at the first round of far-red illumination in the 22-18-21 mutant was essential the same with that in WT, although the rate of

oxidation seems to be somewhat lower. On the other hand, the 22-18-21 mutant showed totally different kinetics of P700 from that of WT in the subsequent rounds of illumination (Figure 8B). The mutant showed very fast oxidation kinetics and did not exhibit slow oxidation phase. Instead, the temporal reduction of P700 was observed in the mutant. Since the rate of charge separation of reaction center or the rate of electron transfer from PSII would not be much different between WT and the mutant, the difference in the oxidation rate of P700 should be due to the different rate of electron transfer from stromal components to the PQ pool. These results suggest that the redox state of the stroma in chloroplast might be altered in the 22-18-21 mutant. In the 37-19-7 mutant, the oxidation kinetics of P700 was less affected than that of the 22-18-21 mutant (Figure 8C), suggesting that the redox state of the stroma in the 37-19-7 mutant might not be affected by far-red-light. To confirm the electron donation to the PQ pool from the stromal donors, P700 kinetics was compared between WT and 22-18-21 (Figure 9). Leaves were illuminated by actinic light (700 □mol photons m^{-2} s^{-1}) under a background of far-red to accumulate reducing equivalent in the stroma. After termination of actinic light illumination, $P700^{+}$ was transiently reduced by electrons from the PQ pool and then P700 was re-oxidized by the background far-red light. The rate of re-oxidation of P700 in the mutant by the background far-red light was much slower than that of WT. These results support that the electron flow from the stroma to the PQ pool is significantly affected in the 22-18-21 mutant.

NDH-dependent cyclic electron flow around PSI is impaired in the 22-18-21 mutant

Figure 10A shows the time course change of chlorophyll fluorescence intensity in WT when dark-adapted leaves were exposed to light. Chlorophyll fluorescence intensity was increased rapidly upon the start of illumination and then lowered gradually to the steady-state level. When the actinic light is switched off after illumination, fluorescence intensity decreased quickly. Subsequently, the fluorescence transiently increased in the dark. This transient increase of chlorophyll fluorescence in the dark has been shown to arise from the reduction of the PQ pool by stromal reductants by NDH-dependent cyclic electron flow around PSI. This transient fluorescence increase was not observed in tobacco *ndhb* mutant (Shikanai et al. 1998, Burrow et al. 1998). The WT leaves showed this transient increase in chlorophyll fluorescence (Figure 10B, upper panel), while leaves of the 22-18-21 mutant did not (Figure 10B, middle panel), indicating that NDH-mediated cyclic electron flow around PSI was impaired. Leaves of the 37-19-7 mutant showed a transient increase in chlorophyll fluorescence (Figure 10B, lower panel), indicating that FQR-dependent cyclic electron flow around PSI is not involved in the transient increase in chlorophyll fluorescence.

The 22-18-21 37-19-7 double mutant shows a more severe defect than either single mutant

There are at least two pathways of cyclic electron transport around PSI. The 37-19-7 mutant was impaired in FQR-dependent cyclic electron flow around PSI as described above. On the other hand, the 22-18-21 mutant appears to have defect in NDH-

dependent pathway. To confirm that the 22-18-21 mutant have defect in different pathway from the defect in the 37-19-7 mutant, the 22-18-21 mutant was crossed with the 37-19-7 mutant. The chlorophyll fluorescence kinetics of the resulting F2 populations was monitored by chlorophyll imaging system (Figure 11A). Most of the plants show similar phenotype (blue lines in Figure 11A) as that of the WT plant. Some plants exhibited the phenotypes (orange and green lines in Figure 11A) observed in either the 22-18-21 plant or the 37-19-7 plant, while one plant exhibited additive phenotype of chlorophyll fluorescence (a pink line in Figure 11A). This result support the conclusion that the 22-18-21 mutant is impaired in different pathway from FQR-dependent cyclic electron flow around PSI; namely an NDH-dependent pathway. The 22-28-21 37-19-7 double mutants were characterized by PAM fluorometry. The formation of NPQ was severely suppressed in the double mutants (Figure 11B). In the 22-18-21 and 37-19-7 mutants, 1-qP was not much affected at any photon flux density (Figure 11C). Since the 1-qP parameter reflects the oxidation state of a primary quinone acceptor in PSII, Q_A, it is suggested that redox state near PQ pool is not disturbed in these mutants. On the other hand, 1-qP is constantly higher in double mutants compared with the single mutants or with WT, indicating that Q_A of double mutants was more reduced. Moreover, the photosynthetic electron transport rate (ETR) of double mutants saturated at a lower level of photon flux densities than the 22-18-21 and 37-19-7 mutants and WT (Figure 11D). These results indicate that cyclic electron flow around PSI is important for photosynthesis just in the case of the *pgr5 crr2* double mutant reported previously (Munekage et al. 2004).

Mapping analysis

The 22-18-21 mutant could not grow in the MS agar containing kanamycin, indicating that the mutation of 22-18-21 was not because of the insertion of the T-DNA. Therefore, to map a gene, I crossed the 22-18-21 mutant with WT of Columbia and Landsberg. CAPS marker in chromosome 1 showed quite lower recombination frequency than other chromosome marker, indicating that the mutation of 22-18-21 is located on chromosome 1. CAPS and SSLP markers in chromosome 1 listed in Table 1 were used for fine mapping. The mutation of the 22-18-21 mutant was closely linked to molecular markers MH6715 and MH6810.

3. The 36-2-20 mutant

Alternative electron transfer pathway is impaired in the 36-2-20 mutant

The 36-2-20 mutant showed different chlorophyll fluorescence kinetics from WT (Figure 1). This suggests that the 36-2-20 mutant has defects in photosynthetic electron transport activity. For further characterization, I measured chlorophyll fluorescence using PAM chlorophyll fluorometry. When compared under normal air condition, the NPQ induction of the 36-2-20 mutant did not show significant difference from that of WT (Table2, Figure 12A). Other photosynthetic parameters (Fv/Fm, 1-qP, Fv'/Fm' and ETR) also did not change in the 36-2-20 mutant even under high light illumination (Table 2). These results suggest that electron transport activity in the 36-2-20 mutant is

hardly affected under normal air condition, although a slight alteration of chlorophyll fluorescence kinetics could be observed in short time range of 12 s (Figure 1).

One possibility is that the alteration of chlorophyll fluorescence kinetics in the 36-2-20 mutant is caused by limitation of alternative electron transport activity which has little impact on the photosynthesis under normal condition. In low CO_2 condition, alternative electron transport should be stimulated because of limitation of CO_2 assimilation. Thus, the time courses of NPQ induction under 0.003% CO_2 condition was compared between the 36-2-20 mutant and WT (Figure 12B). The 36-2-20 mutant showed slightly delayed induction of NPQ, although steady-state NPQ was indistinguishable from that of WT. This suggests that alternative electron transport might be impaired in the 36-2-20 mutant. Cyclic electron flow around PSI, water-water cycle and photorespiration have been referred to as alternative electron transport pathways. In water-water cycle, oxygen was used as an electron acceptor and photorespiration results from the oxygenase reaction catalyzed by Rubisco. Therefore, only cyclic electron flow around PSI should be observed as alternative electron transport activity when concentration of oxygen is low. Figure 12C shows the NPQ induction under O_2 free air condition (N_2 gas with 0.03% CO_2). The NPQ induction within 1 min was delayed in WT compared with normal air condition, suggesting that O_2-dependent electron transport is induced at the early phase of NPQ development under normal air condition. Makino et al (2002) reported that water-water cycle is induced at the early phase of photosynthesis. Even under O_2 free condition, the NPQ induction of the 36-2-20 mutant was slower than that of WT. This suggests that water-

water cycle and photorespiration are not involved in the defects in the 36-2-20 mutant. The ETR induction (Figure 12D) as well as NPQ induction of the 36-2-20 mutant was also slower than that of WT whereas Fv'/Fm' was hardly affected (data not shown). These results suggest that low level of NPQ at the early phase might be caused by insufficient generation of ΔpH due to limited electron transport downstream of PSII; presumably cyclic electron flow around PSI.

hma1 gene is responsible to the phenotype of the 36-2-20 mutant

The 36-2-20 mutant can grow in the presence of kanamycin. The kanamycin-resistance marker and the 36-2-20 phenotype co-segregated, indicating that mutation of 36-2-20 ascribes to T-DNA insertion. I determined DNA sequences flanking T-DNA insertions by TAIL-PCR method. The 36-2-20 mutant turned out to carry a T-DNA insertion in the 10th exson of *hma1* gene (At4g37270) (Figure 13A). The heavy metal P-type ATPases (HMAs), which are responsible for metal transport in plants, compose subfamily of the P-type ATPase. The P-type ATPase family is ubiquitous proteins involved in transport of various compounds. P-type ATPases are divided into five groups based on sequence homology (Axelsen and Palmgren 2001, Baxter, 2003). Type 1_B P-type ATPases are expected to be involved in the transport of heavy metals and can be divided into two further clusters based on their substrate specificity. One cluster (HMA5, 6, 7, 8) has a role in Cu and Ag transport. The second group (HMA1, 2, 3, 4) has been referred to as Zn/Co/Cd/Pb subclass. Among them, HMA2-4 exhibit the most closely related sequences, and their genes appear to arise from gene duplication. Phylogenetic analysis

also reveals that HMA1 is more distantly related to the HMA2/3/4 cluster. HMA1 has eight transmembrane domains, the sixth of which contains Ser-Pro-Cys motif as shown in Figure 13B. This motif is believed to be important for the transport of the metal ion through the membrane. In addition, the N-terminal end has a poly-His domain which might bind heavy metals and serve a role as heavy metal sensor.

The hma1 shows sensitivity to excess Zn

It is reported that single *hma2*, *hma3* and *hma4* mutants do not show an apparent phenotype under normal growth condition (Hussain et al. 2004). They also reported that *hma2 hma4* double mutants showed increased sensitivity to Cd in phytochelatin deficient background (*cad1-3*), although single *hma2*, *hma3* or *hma4* mutants did not show sensitivity to heavy metals. When *hma1* seedlings were grown in MS agar medium, the growth was indistinguishable from that of WT (Figure 14A). This may reflect functional redundancy of heavy metal transporter since Arabidopsis has eight $P1_B$ type ATPase. The *hma1* mutant was tested for sensitivity to excess Zn, Co, Pb and Cd in agar medium. No apparent phenotype was observed in the presence of excess Co, Pb and Cd. On the other hand, *hma1* showed a pale green phenotype and slow growth in the MS medium containing 100 □M $ZnSO_4$ (Figure 14B). This result suggests that *hma1* may accumulate Zn at higher rates because of defect in Zn efflux pump. Thus, the present observation suggests that HMA1 is involved in Zn transport.

Fe addition rescues the hma1 phenotype

In bean plants, it is reported that excess Cu in the growth medium causes Fe deficiency (Patsikka et al. 2002). The addition of Fe lowers the Cu concentration of the leaves. These results suggest that Cu could outcompete Fe in Fe uptake. Similar to this case, excess Zn might cause deficiency of other metal(s) such as Cu, Fe, Mn or Mg that play important role in photosynthesis. To test this hypothesis, I observed growth of *hma1* in various ion-depleted medium. The *hma1* showed pale green phenotype in Fe-depleted medium (Figure 15A). To confirm whether Fe deficiency cause *hma1* phenotype, $FeSO_4$ was supplemented in agar medium containing excess Zn. Growth defect in *hma1* was restored by the addition of $FeSO_4$ (Figure 15B). Furthermore, chlorophyll fluorescence kinetics of *hma1* became close to that of WT when $FeSO_4$ was added to MS medium (Figure 15C). This result suggests that Fe deficiency is the cause of the defect in growth and alternative electron transport in *hma1*.

4. The 38-14-15 mutant

Low wave and high NPQ is induced under high-light condition in the 38-14-15 mutant

Figure 16 shows chlorophyll fluorescence curves of WT and the 38-14-15 mutant using PAM fluorometry. In the 38-14-15 mutant, a transient increase in chlorophyll fluorescence after termination of actinic light was enhanced (Figure 16B, open arrow heads). This phenomenon is ascribed to cyclic electron flow around PSI (Shikanai et al. 1998, Kofer et al. 1998, Burrows et al. 1998). This result suggests that cyclic electron

flow around PSI was enhanced in 38-14-15 under high-light condition. In addition, transient overshoot in chlorophyll fluorescence was also observed after application of saturating light pulses at higher actinic photon flux density in the 38-14-15 mutant (Figure 16B, closed arrow heads). This phenomenon is so called “low-wave”. An involvement of PSI-dependent cyclic electron transport in low-wave phenomenon was suggested from the redox changes of P700 (Tsuyama et al. 2004). From these results, it is suggested that enhanced cyclic electron flow around PSI might cause the low-wave phenomenon in the 38-14-15 mutant. When NPQ induction in the 38-14-15 under high light illumination was compared with that of WT (Figure 17A), NPQ in the first 2 min is much higher in the mutant than that in WT. The high NPQ of the 38-14-15 mutant could be induced by the enhanced cyclic electron flow around PSI.

Alternative electron transport activity in the 38-14-15 mutant

The low-wave phenomenon was detected under chilling stress condition (Larcher and Neuner 1989) and in the absence of either O_2 or CO_2 (Juhler et al. 1993, Miller and Canvin 1989, Klughammer and Schreiber 1994, Heber et al. 1992). Under these stress conditions, availability of CO_2 is limited and relative flow to cyclic electron transfer should be enhanced. Similarly, enhanced cyclic electron transfer of the 38-14-15 mutant might be caused by the defect in other alternative electron transport activity such as photorespiration or water-water cycle. Figure 17B shows the time course of NPQ induction in 38-14-15 and WT under CO_2 free condition. The 38-14-15 mutant showed slightly low NPQ compared to WT. This may suggest that NPQ decreases due to

impairment of alternative electron transport in the 38-14-15 mutant. To examine whether oxygen-mediated alternative pathways were impaired, the NPQ induction was compared between WT and the 38-14-15 mutant under O_2 free condition (N2 gas with 0.03% CO_2). The NPQ induction of the 38-14-15 mutant did not show significant difference from that of WT (Figure 17C). This suggests that oxygen-dependent pathway was impaired in the 38-14-15 mutant. Oxygen can be used both the water-water cycle and photorespiration process. Photorespiration is a consequence of the oxygenation of ribulose-1,5-bisphosphate catalyzed by Rubisco. The ratio of the carboxylation rate to the oxygenation rate is dependent on the ratio of surrounding CO_2 and O_2 concentrations. Thus, photorespiration reaction can be suppressed under high CO_2 condition because Rubisco catalyses only carboxylation under such condition. To examine whether photorespiration pathway was impaired in the 38-14-15 mutant, NPQ induction of the 38-14-15 mutant under high CO_2 condition (0.2% CO_2) was compared to that of WT. As shown in Figure 17D, NPQ induction of the 38-14-15 mutant was almost the same as that of WT. This result suggests that photorespiration pathway was impaired in the 38-14-15 mutant.

Photorespiration is important mechanism for photosynthesis

It is suggested that photorespiration could serve as electron sinks under high light condition. When photosynthetic parameters were determined with increasing photon flux densities, 1-qP is higher in the 38-14-15 mutant than in WT at a photon flux density of more than 1000 □mol photons m^{-2} s^{-1}, indicating that Q_A was more reduced than WT

under high light condition (Figure 18 A). Corresponding to more reduced Q_A in the mutant, ETR was lower in the mutant at high photon flux densities (Figure 18B). The difference between WT and the 38-14-15 mutant in the rate of electron transfer at high photon flux densities must be due to photorespiration which is potential sink of electrons.

Mapping analysis

The 38-14-15 mutant could grow in the presence of kanamycin. However, the kanamycin-resistance marker and the phenotype of 38-14-15 did not co-segregate, indicating that the mutation was not due to the insertion of the T-DNA. Therefore, I examined map-based cloning method. One CAPS marker in chromosome 4, G4539, showed quite lower recombination frequency than other chromosome marker, indicating that the 38-14-15 mutation was mapped to chromosome 4. Additional CAPS and SSLP markers in chromosome 4 listed in Table 1 were used for fine mapping. The 38-14-15 mutation was closely linked to molecular markers FCA11 and MH8100.

DISCUSSION

1. Cyclic electron flow around PSI

The 37-19-7 mutant as a weak allele of pgr5

In the present study, I isolated two mutants (37-19-7, 22-18-21) defective in PSI-dependent cyclic electron transport. The 37-19-7 mutant carried a mutation in *pgr5* gene which is involved in FQR-dependent cyclic pathway. Chlorophyll fluorescence analysis shown in Figure 10 indicates that the 22-18-21 mutant is defective in NDH-dependent cyclic electron flow around PSI. The 22-18-21 37-19-7 double mutant did not show any visible phenotype, though it showed more severe defect of the NPQ, 1-qP and ETR than each single mutant (Figure 11). On the other hand, the *pgr5 crr2* double mutants similarly defective in both PSI-dependent cyclic pathways showed the decrease in the growth rate and in the chlorophyll content even when plants are grown under weak light condition (Munekage et al. 2004). This discrepancy may be due to the difference in the phenotype of *pgr5* and the 37-19-7 mutant. In *pgr5*, it was shown that ETR was lower than that of WT at higher photon flux densities. On the other hand, ETR in the 37-19-7 mutant was indistinguishable from that of WT (Table 2). Additionally, photon flux density dependence of NPQ and the redox state of P700 seem to be more affected in *pgr5* than in the 37-19-7 mutant. PGR5 consists of 133 amino acids as shown in Figure 4. In *pgr5,* glycine at position 130 is replaced with serine, resulting in a null mutant. In the 37-19-7 mutant, asparagine at position 125 was substituted for a lysine. Judging from these results, the 37-19-7 mutant should be a weak allele of *pgr5* and Gyl^{130} in

PGR5 seems to be more important for its function than Asp^{125}.

Switching of two cyclic pathways

There were several phenotypic differences between the 22-18-21 mutant and the 37-19-7 mutant, dependent on the light intensity and quality. As shown in Figure 10A, chlorophyll fluorescence increases transiently after termination of actinic light due to the reduction of the PQ pool by the electron flow from NDH-dependent cyclic pathway. This increase in chlorophyll fluorescence in the dark was absent in the 22-18-21 mutant (NDH-defective mutant), but present in the 37-19-7 mutant (FQR-defective mutant) as shown in Figure 10B. In addition, the P700 oxidation kinetics of the 22-18-21 mutant by far-red light is quite different from WT, whereas the 37-19-7 mutant did not show significant difference from WT (Figure 8). These results suggest that NDH-mediated cyclic electron flow preferentially function in the dark and under far-red light. On the other hand, under white actinic light, the 22-18-21 mutant did not show significant difference from WT (Figure 7), whereas the P700 was reduced with increasing photon flux densities in the 37-19-7 mutant (Figure 3). This suggests that FQR-dependent pathway mainly acts under white actinic light. It is reported that electron flow from NADPH to the PQ pool operates only under the condition that $NADP^+$/NADPH pool is reduced and the PQ pool is oxidized (Tsujimoto et al. 1980, Hosler and Yocum 1985). The PQ pool locates between PSII and cytochrome b_6f complexes. The PQ pool becomes more reduced under high actinic light and oxidized in the dark or under far-red light. It is expected that FQR-dependent pathway dominate when the PQ pool is more

reduced. Adversely, NDH-dependent pathway might dominate when the PQ pool is oxidized. Thus, two pathways of cyclic electron flow around PSI must respond differently to the redox state of the PQ pool.

Several distinct roles of NDH complex

The oxidation kinetics of P700 in the 22-18-21 mutant shown in Figure 9 was different from that of previously reported tobacco Δ*ndhB* plants (Shikanai et al. 1998). In the 22-18-21 mutant, the re-oxidation of P700 with far-red light was much slower than that of WT. On the other hand, re-oxidation was much faster in ΔndhB than in WT. In addition, the 22-18-21 mutant showed decreased NPQ with increasing light intensity, whereas Δ*ndhB* and *crr2* mutant does not have any defect in photosynthetic electron transport. Why the 22-18-21 mutant shows different phenotype from previously identified NDH mutants?

One plausible reason is multiple functions of NDH complexes. In cyanobacteria and higher plants, NDH complexes have been reported to have distinct functions (chlororespiration and PSI cyclic electron flow). Herranen et al (2004) reported the presence of four different complex containing NDH subunits in *Synechocystis* sp. PCC6803. Among them, NDH-1M and NDH-1L are different protein complexes with distinct function (Zhang et al. 2004). Although subunit composition of the chloroplast NDH complexes is not elucidated at present in Arabidopsis, several types of complexes may have distinct functions similar to cyanobacteria. This multiple functions of NDH complexes might lead to the variation of phenotypes. Recently, novel

subunits of NDH (NDH-M, -N, -O) have been identified in Arabidopsis (Rumeau et al. 2005). The newly identified Arabidopsis *ndhm*, *ndhn* and *ndho* mutants show slight increase in NPQ at higher intensity light (Rumeau et al. 2005), which is different phenotype from *crr2* mutant. This observation also supports my hypothesis.

The *pgr5* mutant has defect in electron transport at high photon flux densities. On the other hand, ΔndhB and *crr2* is unaffected in photosynthetic electron transport at any photon flux densities. Therefore, the NDH-mediated cyclic electron pathway has been thought to be not essential for photosynthesis. However, *pgr5 crr2* double mutant showed severe defects than single *pgr5* mutant, implying the importance of NDH-mediated cyclic electron flow. In the present study, the 22-18-21 mutant showed low NPQ compared with WT under high light condition due to the inability of keeping high NPQ (Figure 5, 6). This observation raised the possibility that NDH-mediated pathway is also important for efficient photosynthesis. Further analysis of the 22-18-21 mutant including identification of the mutated gene may dissect the physiological role of NDH-dependent cyclic electron flow around PSI.

2. Homeostasis of metal ions in chloroplast

HMA1 functions as a Zn transporter

In this study, I demonstrated that HMA1, a $P1_B$-ATPase, is a novel protein involved in Zn transport. The $P1_B$-ATPases have been identified in a wide range of organism. However, eukaryotes other than plants appear to have a limited number of $P1_B$ ATPase

(one or two) and those have been identified as transporters specific to Cu/Ag. On the other hand, Arabidopsis has eight genes encoding $P1_B$-ATPases and four of which are involved in Zn/Cd/Pb/Co transport. Some of HMAs are involved in delivering heavy metal ions to specific proteins, like is the case for PAA1 (HMA6) (Shikanai et al. 2003) and RAN1 (HMA7) (Hirayama et al. 1999, Woeste and Kieber 2000). HMA6 is shown to be involved in the delivery of Cu to chloroplast Cu proteins, Cu/Zn superoxide dismutase and plastocyanin. HMA7 has been identified as a transporter to be involved in the biogenesis of ethylene receptor.

Other role of HMAs is suggested to be involved in accumulation of heavy metal ions in subcellular compartments and ensuring that the levels inside the cells do not reach toxic levels. The HMA2 is shown to be involved in cytoplasmic Zn homeostasis (Eren and Arguello 2004). The *hma2* mutant accumulates Zn and Cd when plants are exposed to high Zn and Cd concentrations. HMA3 expression enhances Cd/Pb tolerance in yeast Cd/Pb-sensitive strain (Gravot et al. 2004), suggesting the involvement in Cd/Pb transport. HMA4 is suggested to function root to shoot translocation of Zn and Cd. HMA4 also confers Zn tolerance to E. coli *zntA* mutant that is highly sensitive to high Zn concentration (Mills et al. 2003). However, there has been no report on the function of HMA1 so far. In this study, I observed that the *hma1* showed sensitivity to excess Zn (Figure 14). This suggests that HMA1 acts as Zn efflux pump to protect from Zn toxicity. The analysis of GFP fusion protein suggests that HMA2 and HMA4 are localized to plasma membrane and HMA3 might exist in vacuole. HMA1 is predicted to have a chloroplast transit signal sequences by ChloroP

(www.cbs.dtu.dk/services/ChloroP/). Additionally, HMA1 is found to be located in chloroplast envelope membranes by proteomic analysis (Ferro et al. 2003). These results support that HMA1 functions as Zn transporter functioning in chloroplasts.

Accumulation of excess Zn results in the deficiency of Fe

The *hma1* showed pale green phenotype in Fe-depleted medium (Figure 14A). Moreover, Fe addition to the growth medium rescued the pale green phenotype of *hma1* caused by excess Zn (Figure 15B). This observation is consistent with the suggestion that Zn toxicity induces chlorosis, probably via competition with Fe and Mg (Woolhouse 1983, Marschner 1995). The *hma1* also showed slightly pale green color compared with WT when the Mg concentration in the growth medium was decreased (data not shown). Another plausible mechanism leading to the Fe deficiency is the inhibition of Fe transporter. Fe is transported into root via IRT1 protein in Arabidopsis (Eide et al. 1996; Vert et al. 2002). It is reported that IRT1 protein levels decline by addition of excess Zn (Connolly et al. 2002). In *hma1*, Fe deficiency might be caused by the decrease of IRT1 protein because of accumulation of Zn. Fe deficiency is reported to cause the low activities of antioxidative enzyme (Iturbe-Ormaetxe et al. 1995). Oxidative stress caused by Fe deficiency might lead to reduced leaf chlorophyll concentration.

Role of Zn in photosynthesis

Zn is essential micronutrients for plant growth. Zn plays an important role in several

plant metabolic processes; it activates enzymes and is involved in protein synthesis and carbohydrate, nucleic acid and lipid metabolism. Zn accumulation or deficiency is known to cause alterations in vital growth processes (Welch 1995, Bonnet et al. 2000). In chloroplasts, Zn is also needed as a cofactor of Cu/Zn superoxide dismutase and carbonic anhydrase. Despite of its importance, the effect of Zn homeostasis on photosynthesis is poorly understood. There are some Arabidopsis mutants with altered photosynthetic activity due to defects in heavy metal homeostasis. Varotto et al (2002) isolated *irt1* mutant based on a decrease in the effective quantum yield of PSII. They demonstrated that IRT1 is necessary for iron homeostasis and efficient photosynthesis. The *paa1* (*hma6*) mutant shows a high chlorophyll fluorescence phenotype arising from impaired photosynthetic electron transport due to a defect in Cu transport to chloroplast (Shikanai et al 2003).

Chlorophyll fluorescence analysis suggests that *hma1* is impaired in alternative electron pathway, presumably cyclic electron transport around PSI (Figure 12). This impairment of electron transport might be explained by the Fe deficiency. As shown in Figure 15C, addition of extra Fe was restored the phenotype of chlorophyll fluorescence. This supports that Fe deficiency leads to the alteration of electron transport in *hma1*. Fe is essential metal for photosynthesis. PSI and cytochrome b_6f complex contain iron-sulfur proteins. In addition, NDH complexes that catalyze cyclic electron flow around PSI also have iron-sulfur clusters. Fe deficiency might affect these proteins, resulting in the inhibition of cyclic electron flow around PSI *hma1*. Thus, Zn homeostasis maintained by HMA1 is important for efficient photosynthesis.

3. Photorespiration

Cyclic electron transfer around PSI is enhanced by impairment of photorespiration

In the 38-14-15 mutant, a transient overshoot in chlorophyll fluorescence upon saturating light pulse was detected as shown in Figure 16B. Larcher and Neuner (1989) first reported this phenomenon and named it “low-wave”. However, the mechanism of this brief fluorescence decreases has not been fully understood. Hagen et al. (1992) ascribed low-wave to transiently increased photochemical quenching caused by electron transport from PSII to PSI. Xylander and Hagen (2002) proposed that low-wave represented a deprivation of bicarbonate in PSII complex. Low wave phenomenon was often detected under temperature stress condition and low CO_2 and O_2 condition. It has been suggested that the capacity for cyclic electron flow around PSI may be enhanced after light-chilling stress in cucumber leaves (Sonoike 1999) and under low CO_2 condition in cyanobacteria (Deng, 2003). Recently, Tsuyama et al (2004) showed that low-wave was accompanied by the change of the redox state of PSI. They suggest that low wave is induced by increased NPQ due to cyclic electron flow around PSI. The low-wave phenomenon observed in the 38-14-15 mutant might be also explained by the enhanced cyclic electron flow around PSI judging from the increase in chlorophyll fluorescence after termination of actinic light (Figure 16). In the 38-14-15 mutant, linear electron transport was limited due to inhibition of photorespiration pathway. Thus, the present observation suggests that limitation of electron acceptor caused by the

impairment of photorespiration leads to the enhancement of PSI cyclic electron transport.

Photorespiration and proton gradient

NPQ, which competes with photochemistry, must be strictly controlled to avoid losses in photosynthetic efficiency. In the 38-14-15 mutant, aberrant high NPQ was induced upon high light illumination as shown in Figure 17A. The high NPQ was observed in Arabidopsis *dpa1* mutant lacking ATPase □subunit (Bosco et al. 2004). The induction of NPQ requires a lumenal acidification of thylakoid membrane. In *dpa1*, the disruption of ATP synthase results in the accumulation of a large proton gradient through thylakoid membrane, leading to the induction of high NPQ. Thus, a large pH gradient leads to strong induction of NPQ. Photorespiration requires more ATP and NADPH than for the CO_2 fixation. Since ATP could not be used for photorespiration process in the 38-14-15 mutant, a large proton gradient across the thylakoid membrane may generate, leading to increased NPQ activity. A proton gradient is also generated by cyclic electron flow around PSI. Enhancement of cyclic electron flow around PSI might also result in the high NPQ. As shown in Figure 17A, however, high NPQ was canceled during illumination and steady-state NPQ level was indistinguishable from WT with actinic light of 700 □mol photons m^{-2} s^{-1}. A large proton gradient generated in the 38-14-15 mutant might not be dissipated as quickly as WT, leading to the delay in relaxation of NPQ. 1-qP is higher in the 38-14-15 mutant than in WT at a photon flux density of more than 1000 □mol photons m^{-2} s^{-1} (Figure 18A). The NPQ is important mechanism for

plants to prevent photodamage. However, it is suggested that NPQ reaches a maximum well before irradiances reached saturation. Therefore, other mechanisms than NPQ are required in maintaining the proper redox state of electron acceptors under such condition. Photorespiration might function as an electron sink with much higher irradiances.

Physiological role of photorespiration

Photorespiration is suggested to serve as electron sink under high light condition, because excess energy is dissipated by consumption of NADPH and ATP through photorespiration. It is reported that the transgenic tobacco expressing photorespiratory enzyme had increased tolerance to a high-light intensity (Kozaki and Takeba 1996). The ETR of the 38-14-15 mutant saturated at lower photon flux density than that of WT (Figure 18B). The present observation indicates that photorespiration is important mechanism for photoprotection. Photorespiration also provides metabolites such as glycine and serine. Glycine is used in the process of glutathione synthesis. Since glutathione is a component of antioxidant in higher plants (Noctor and Foyer 1998), photorespiration process may contribute additional protection against high light by supplying glycine.

Even if the photorespiration is important for the plant survival under changing light environments, the photorespiration itself is the process to consume ATP and NADPH wastefully. Rubisco is inefficient enzyme for CO_2 fixation because of its oxygenation activity. Therefore, suppression of photorespiraion might lead to the

increase in CO_2 fixation activity. Thus, there is a possibility that the mutant defect in the photorespiration shows high productivity under artificially controlled environment in industrial agriculture. Future identification of the gene responsible for the phenotype of the 38-14-15 mutant may lead to the exploration of such possibility.

CONCLUSION

In the present study, I isolated four novel Arabidopsis mutants (37-19-7, 22-18-21, 36-2-20, 38-14-15) by monitoring the time course changes of chlorophyll fluorescence intensity. The impaired site of isolated mutants in this study was shown in Figure 19. The characterization of these mutants revealed some novel features in alternative electron pathways as follows. (1) Two PSI-dependent cyclic electron pathways differently respond to the redox state of the PQ pool. FQR-dependent pathway dominates when the PQ pool is more reduced. NDH-dependent pathway mainly functions when the PQ pool is oxidized. (2) The HMA1, a $P1_B$-type ATPase, is involved in Zn transport. High Zn concentration leads to the Fe deficiency in chloroplast, leading to the alteration in PSI cyclic electron transport and to leaf chlorosis. Thus, Zn homeostasis within chloroplast is essential for photosynthesis. (3) The impairment in photorespiration leads to the enhancement of cyclic electron flow around PSI. Photorespiration is important mechanism against high light stress.

REFERENCES

Anderson, J.M., Choe, W.S, and Park, Y.I. (1995). The grand design of photosynthesis: acclimation of the photosynthetic apparatus to environmental cues. Photosyn. Res. **46,** 129-139.

Aro, E.M., McCaffery, S., and Anderson, J.M. (1993). Photoinhibition and D1 Protein Degradation in Peas Acclimated to Different Growth Irradiances. Plant Physiol. **103,** 835-843.

Asada, K. (2000). The water-water cycle as alternative photon and electron sinks. Philos. Trans. R Soc. Lond. B Biol. Sci. **355,** 1419-1431.

Axelsen, K.B., and Palmgren, M.G. (2001). Inventory of the superfamily of P-type ion pumps in Arabidopsis. Plant Physiol. **126,** 696-706.

Bailey, S., Walters, R.G., Jansson, S., and Horton, P. (2001). Acclimation of *Arabidopsis thaliana* to the light environment: the existence of separate low light and high light responses. Planta **213,** 794-801.

Baroli, I., and Niyogi, K.K. (2000). Molecular genetics of xanthophyll-dependent photoprotection in green algae and plants. Philos. Trans. R. Soc. Lond. B. Biol. Sci. **355,** 1385-1394.

Baxter, I., Tchieu, J., Sussman, M.R., Boutry, M., Palmgren, M.G., Gribskov, M., Harper, J.F., and Axelsen, K.B. (2003). Genomic comparison of P-type ATPase ion pumps in Arabidopsis and rice. Plant. Physiol. **132,** 618-628.

Bell, C.J., and Ecker, J.R. (1994). Assignment of 30 microsatellite loci to the linkage

map of *Arabidopsis*. Genomics **19,** 137-144.

Bonnet, M., Camares, O., and Veisseire, P. (2000). Effects of zinc and influence of *Acremonium lolii* on growth parameters, chlorophyll a fluorescence and antioxidant enzyme activities of ryegrass (*Lolium perenne* L. cv Apollo). J. Exp. Bot. **51,** 945-953.

Bosco, C.D., Lezhneva, L., Biehl, A., Leister, D., Strotmann, H., Wanner, G., and Meurer, J. (2004). Inactivation of the chloroplast ATP synthase gamma subunit results in high non-photochemical fluorescence quenching and altered nuclear gene expression in *Arabidopsis thaliana*. J. Biol. Chem. **279,** 1060-1069.

Blackwell, R.D., Murray, A.J.S., and Lea, P.J. (1990). Photorespiratory mutants of the mitochondrial conversion of glycine to serine. Plant. Physiol. **94,** 1316-1322.

Burrows, P.A., Sazanov, L.A., Svab, Z., Maliga, P., and Nixon, P.J. (1998). Identification of a functional respiratory complex in chloroplasts through analysis of tobacco mutants containing disrupted plastid *ndh* genes. Embo J. **17,** 868-876.

Chow, W.S., Melis, A., and Anderson, J.M. (1990). Adjustments of photosystem stoichiometry in chloroplasts improve the quantum efficiency of photosynthesis. Proc. Natl. Acad. Sci. U S A. **87,** 7502-7506.

Connolly, E.L., Fett, J.P., and Guerinot, M.L. (2002). Expression of the IRT1 metal transporter is controlled by metals at the levels of transcript and protein

accumulation. Plant Cell **14,** 1347-1357.

Demmig-Adams, B. (1990). Carotenoids and photoprotection in plants; a role for the xanthophyll zeaxanthin. Biochem. Biophys. Acta **1990,** 1-24.

Deng, Y., Ye, J., and Mi, H. (2003). Effects of low CO_2 on NAD(P)H dehydrogenase, a mediator of cyclic electron transport around photosystem I in the cyanobacterium *Synechocystis* PCC6803. Plant Cell Physiol. **44,** 534-540.

Douce, R., and Neuburger, M. (1999). Biochemical dissection of photorespiration. Curr. Opin. Plant Biol. **2,** 214-222.

Eide, D., Broderius, M., Fett, J., and Guerinot, M.L. (1996). A novel iron-regulated metal transporter from plants identified by functional expression in yeast. Proc. Natl. Acad. Sci. U S A **93,** 5624-5628.

Eren, E., and Arguello, J.M. (2004). Arabidopsis HMA2, a divalent heavy metal-transporting PIB-type ATPase, is involved in cytoplasmic Zn^{2+} homeostasis. Plant Physiol. **136,** 3712-3723.

Farquar, G.D., Von Gaemmerer, S., and Berry, J.A. (1980). A biochemical model of photosynthetic CO_2 assimilation in leaves of C_3 species. Planta **149**, 78-90.

Ferro, M., Salvi, D., Brugiere, S., Miras, S., Kowalski, S., Louwagie, M., Garin, J., Joyard, J., and Rolland, N. (2003). Proteomics of the chloroplast envelope membranes from *Arabidopsis thaliana*. Mol. Cell Proteomics **2**, 325-345

Gravot, A., Lieutaud, A., Verret, F., Auroy, P., Vavasseur, A., and Richaud, P. (2004). AtHMA3, a plant $P1_B$-ATPase, functions as a Cd/Pb transporter in yeast. FEBS Lett. **561,** 22-28.

Hagen, C., Bornman, J.F., and Braune, W. (1992). Reversible lowerng of modulated chlorophyll fluorescence after saturating flashes in *Haematococcus lacustris* (Volvocales) at room temperature. Physiological Plantarum **86,** 593-599.

Hashimoto, M., Endo, T., Peltier, G., Tasaka, M., and Shikanai, T. (2003). A nucleus-encoded factor, CRR2, is essential for the expression of chloroplast ndhB in *Arabidopsis*. Plant J. **36,** 541-549.

Heber, U., Bukhov, N.G., Shuvalov, V.A., Kobayashi, Y., and Lange, O.L. (2001). Protection of the photosynthetic apparatus against damage by excessive illumination in homoiohydric leaves and poikilohydric mosses and lichens. J. Exp. Bot. **52,** 1999-2006.

Herranen, M., Battchikova, N., Zhang, P., Graf, A., Sirpio, S., Paakkarinen, V., and Aro, E.M. (2004). Towards functional proteomics of membrane protein complexes in *Synechocystis* sp. PCC 6803. Plant Physiol. **134,** 470-481.

Hever, U., Neimanis, S., Siebke, K., Schonknecht,G., and Katona, E. (1992). Chloroplast energization and oxidation of P700/plastocyanin in illuminated leaves at reduced levels of CO_2 or oxygen. Photosynth. Res. **34,** 433-447.

Hirayama, T., Kieber, J.J., Hirayama, N., Kogan, M., Guzman, P., Nourizadeh, S., Alonso, J.M., Dailey, W.P., Dancis, A., and Ecker, J.R. (1999). RESPONSIVE-TO-ANTAGONIST1, a Menkes/Wilson disease-related copper transporter, is required for ethylene signaling in *Arabidopsis*. Cell **97,** 383-393.

Hosler, J.P., and Yocum, C.F. (1985). Evidence for two cyclic photophosphorylation reactions concurrent with ferredoxin-catalyzed non-cyclic electron transport.

Biochemi. Biophysi. Acta **808,** 21-31.

Huber, S.C., and Edwards, G.E. (1976). Studies on the pathway of cyclic electron flow in mesophyll chloroplasts of a C_4 plant. Biochim. Biophys. Acta **449,** 420-433.

Hussain, D., Haydon, M.J., Wang, Y., Wong, E., Sherson, S.M., Young, J., Camakaris, J., Harper, J.F., and Cobbett, C.S. (2004). P-type ATPase heavy metal transporters with roles in essential zinc homeostasis in Arabidopsis. Plant Cell **16,** 1327-1339.

Iturbe-Ormaetxe, I., Moran, J. F., Arresse-Igor, C., Gogorcena, Y., Klucas, R. V., Becana, M. (1995). Activated oxygen and antioxidant defenses in iron-deficient pea plants. Plant Cell Environ. **18**, 421-429.

Joliot, P., and Joliot, A. (2002). Cyclic electron transfer in plant leaf. Proc. Natl. Acad. Sci. U S A. **99,** 10209-10214.

Juhler, R.K., Miller, M., Simpson, D., and Cox, R.P. (1993). Chlorophyll fluorescence transients in a barley mutant lacking Photosystem. I. Photosynth. Res. **35**, 305-310.

Klughammer, C., and Schreiber, U. (1994). An improved method, using saturating light pulse, for the determination of Photosystem I quantum yield via $P700^+$-absorbance changes at 830 nm. Planta **192**, 261-268.

Kofer, W., Koop, H.U., Wanner, G., and Steinmuller, K. (1998). Mutagenesis of the genes encoding subunits A, C, H, I, J and K of the plastid NAD(P)H-plastoquinone-oxidoreductase in tobacco by polyethylene glycol-mediated

plastome transformation. Mol. Gen. Genet. **258,** 166-173.

Konieczny, A., and Ausubel, F.M. (1993). A procedure for mapping *Arabidopsis* mutations using co-dominant ecotype-specific PCR-based markers. Plant J. **4,** 403-410.

Kozai, A., and Takeba, G. (1996). Photorespiration protects C_3 plants from photooxidation. Nature **384,** 557-560.

Larcher, W., and Neuner, G. (1989). Cold-induced sudden reversible lowering of in vivo chlorophyll fluorescence after saturating light pulse. A sensitive marker for chilling susceptibility. Plant Physiol. **89**, 740-742.

Li, X.P., Bjorkman, O., Shih, C., Grossman, A.R., Rosenquist, M., Jansson, S., and Niyogi, K.K. (2000). A pigment-binding protein essential for regulation of photosynthetic light harvesting. Nature **403,** 391-395.

Liu, Y.G., Mitsukawa, N., Oosumi, T., and Whittier, R.F. (1995). Efficient isolation and mapping of *Arabidopsis thaliana* T-DNA insert junctions by thermal asymmetric interlaced PCR. Plant J. **8,** 457-463.

Makino, A., Miyake, C., and Yokota, A. (2002). Physiological functions of the water-water cycle (Mehler reaction) and the cyclic electron flow around PSI in rice leaves. Plant Cell Physiol. **43,** 1017-1026.

Marschner, H. (1995). Mineral nutrition of higher plants. Ed 2, Academic Press, London.

Meurer, J., Meierhoff, K., and Westhoff, P. (1996). Isolation of high-chlorophyll-fluorescence mutants of *Arabidopsis thaliana* and their characterization by

spectroscopy, immunoblotting and northern hybridization. Planta **198,** 385-396.

Miller, A.G., and Canvin, D.T. (1989). Glycolaldehyde inhibits fixation CO_2 fixation in the cyanobacterium *Synechococcus* UTEX 625 without inhibiting the accumulation of inorganic carbon or the associated quenching of chlorophyll a fluorescence. Plant Physiol. **91,** 1044-1049.

Mills, R.F., Krijger, G.C., Baccarini, P.J., Hall, J.L., and Williams, L.E. (2003). Functional expression of AtHMA4, a $P1_B$-type ATPase of the Zn/Co/Cd/Pb subclass. Plant J. **35,** 164-176.

Muller, P., Li, X.P., and Niyogi, K.K. (2001). Non-photochemical quenching. A response to excess light energy. Plant Physiol. **125,** 1558-1566.

Murray, A.J.S., Blackwell, R.D., and Lea, P.J. (1989). Metabolism of hydroxypyruvate in a mutant of barley lacking NADH-dependent hydroxypyruvate reductase, an import photorespiratory enzyme activity. Plant. Physiol. **91,** 395-400.

Murray, A.J.S., Blackwell, R.D., Joy, K.W., and Lea, P.J. (1987). Photorespiratory N-donors, aminotransferase specificity and photosynthesis in a mutant of barley deficient in serine:glyoxylate aminotransferase activity. Planta **172,** 106-113.

Munekage, Y., Hashimoto, M., Miyake, C., Tomizawa, K., Endo, T., Tasaka, M., and Shikanai, T. (2004). Cyclic electron flow around photosystem I is essential for photosynthesis. Nature **429,** 579-582.

Munekage, Y., Hojo, M., Meurer, J., Endo, T., Tasaka, M., and Shikanai, T. (2002).

PGR5 is involved in cyclic electron flow around photosystem I and is essential for photoprotection in Arabidopsis. Cell **110,** 361-371.

Munekage, Y., Takeda, S., Endo, T., Jahns, P., Hashimoto, T., and Shikanai, T. (2001). Cytochrome b_6f mutation specifically affects thermal dissipation of absorbed light energy in *Arabidopsis*. Plant J. **28,** 351-359.

Niyogi, K.K. (1999). PHOTOPROTECTION REVISITED: Genetic and Molecular Approaches. Annu Rev Plant Physiol. Plant Mol. Biol. **50,** 333-359.

Niyogi, K.K., Bjorkman, O., and Grossman, A.R. (1997). Chlamydomonas Xanthophyll Cycle Mutants Identified by Video Imaging of Chlorophyll Fluorescence Quenching. Plant Cell **9,** 1369-1380.

Noctor, G., and Foyer, C.H. (1998). Ascorbate and glutathione: keeping active oxygen under control. Annu. Rev. Plant Physiol. Plant Mol. Biol. **49,** 249-279.

Patsikka, E., Kairavuo, M., Sersen, F., Aro, E.M., and Tyystjarvi, E. (2002). Excess copper predisposes photosystem II to photoinhibition in vivo by outcompeting iron and causing decrease in leaf chlorophyll. Plant Physiol. **129,** 1359-1367.

Rumeau, D., Becuwe-Linka, N., Beyly, A., Louwagie, M., Garin, J., and Peltier, G. (2005). New Subunits NDH-M, -N, and -O, Encoded by Nuclear Genes, Are Essential for Plastid Ndh Complex Functioning in Higher Plants. Plant Cell **17,** 219-232.

Schreiber, U., and Bilger, Z. (1993). Progress in chlorophyll fluorescence research: major development during the last years in retrospect. Progress in Botany **54,** 151-173.

Shikanai, T., Muller-Moule, P., Munekage, Y., Niyogi, K.K., and Pilon, M. (2003). PAA1, a P-type ATPase of Arabidopsis, functions in copper transport in chloroplasts. Plant Cell **15,** 1333-1346.

Shikanai, T., Endo, T., Hashimoto, T., Yamada, Y., Asada, K., and Yokota, A. (1998). Directed disruption of the tobacco *ndhB* gene impairs cyclic electron flow around photosystem I. Proc. Natl. Acad. Sci. U S A. **95,** 9705-9709.

Shikanai, T., Munekage, Y., Shimizu, K., Endo, T., Hashimoto, T. (1999). Identification and characterization of *Arabidopsis* mutants with reduced quenching of chlorophyll fluorescence. Plant Cell Physiol. **40,** 1134-1142.

Smirnoff, N. (2000). Ascorbate biosynthesis and function in photoprotection. Philos. Trans. R. Soc. Lond. B. Biol. Sci. **355,** 1455-1464.

Somerville, C.R., and Ogren, W.L. (1979). A phosphoglycolate phosphatase-deficient mutant of *Arabidopsis*. Nature **280,** 833-836.

Somerville, C.R., and Ogren, W.L. (1980). Inhibition of photosynthesis in *Arabidopsis* mutants laking leaf glutamate synthase activity. Nature **286,** 257-259.

Somerville, C.R., and Ogren, W.L. (1981). Photorespiration-deficient mutants of *Arabidopsis thaliana* lacking mitochondrial serine transhydroxymethylase activity. Plant. Physiol. **67,** 666-671.

Somerville, C.R., and Ogren, W.L. (1982). Mutants of the cruciferous plant *Arabidopsis thaliana* lacking glycine decarboxylase activity. Biochem. J. **202,** 373-380.

Sonoike, K. (1999). The different roles of chilling temperatures in the photoinhibition

of Photosystem I and Photosystem II J Photochem. Photobiol. B:Biol. **48**, 136-141.

Tsujimoto, H.Y., Hiyama, T., and Arnon, D.I. (1990). Affinity of ferredoxin for electrons from water and the regulation of cyclic photophosphorylation. Biochem. Biophys. Res. Commun. **93**.

Tsuyama, M., Shibata, M., Kawazu, T., and Kobayashi, Y. (2004). An analysis of the mechanism of the low-wave phenomenon of chlorophyll fluorescence. Photosyn. Res. **81,** 67-76.

Varotto, C., Maiwald, D., Pesaresi, P., Jahns, P., Salamini, F., and Leister, D. (2002). The metal ion transporter IRT1 is necessary for iron homeostasis and efficient photosynthesis in *Arabidopsis thaliana*. Plant J. **31,** 589-599.

Verret, F., Gravot, A., Auroy, P., Leonhardt, N., David, P., Nussaume, L., Vavasseur, A., and Richaud, P. (2004). Overexpression of AtHMA4 enhances root-to-shoot translocation of zinc and cadmium and plant metal tolerance. FEBS Lett. **576,** 306-312.

Vert, G., Grotz, N., Dedaldechamp, F., Gaymard, F., Guerinot, M.L., Briat, J.F., and Curie, C. (2002). IRT1, an Arabidopsis transporter essential for iron uptake from the soil and for plant growth. Plant Cell **14,** 1223-1233.

Welch, R.M. (1995). Micro nutrient nutrition of plants. Crit. Rev. Plant Sci. **14,** 49-82

Wingler, A., Lea, P.J., Quick, W.P., and Leegood, R.C. (2000). Photorespiration: metabolic pathways and their role in stress protection. Philos. Trans. R. Soc. Lond. B. Biol. Sci. **355,** 1517-1529.

Woeste, K.E., and Kieber, J.J. (2000). A strong loss-of-function mutation in RAN1 results in constitutive activation of the ethylene response pathway as well as a rosette-lethal phenotype. Plant Cell **12,** 443-455.

Woolhouse, H.P. (1983) Toxicity and tolerance in the responses of plants to metals. Encyclopedia of Plant Physiology, New Series, 1983, Vol 12C, Physiological Plant EcologyIII, Responses to the Chemical and Biological Environment, Berlin.

Yamamoto, H.Y., Nakayama, T.O., and Chichester, C.O. (1962). Studies on the light and dark interconversions of leaf xanthophylls. Arch. Biochem. Biophys. **97,** 168-173.

Xylander, M., and Hagen, C. (2002). 'Low-waves' in chlorophyll fluorescence kinetics indicate deprivation of bicarbonate. Photosyn. Res. **72,** 255-262.

Zhang, P., Battchikova, N., Jansen, T., Appel, J., Ogawa, T., and Aro, E.M. (2004). Expression and functional roles of the two distinct NDH-1 complexes and the carbon acquisition complex NdhD3/NdhF3/CupA/Sll1735 in *Synechocystis* sp PCC 6803. Plant Cell **16,** 3326-3340.

TABLES

Table 1. CAPS and SSLP markers used in this study.

Marker name	Type of marker	Enzyme	Primer sequence (5')	Primer sequence (3')	Chromosome
NCC1	CAPS	RsaI	AAGTTATAAGGCATTAGAATCATAATC	GTCCTATCTCTACGATGTGGATG	1
ML	CAPS	SnabI	CGGAAACACGAAGCTGATGAGTTGGG	CGAGAACAAAATGTGTACGGTGTG	2
BGL1	CAPS	RsaI	TTATCACCATAACGTCTCCC	TCTTCTCGGTCTATTCTTCG	3
G4539	CAPS	HindIII	GGACGTAGAATCTGAGAGCTC	GGTCATCCGTTCCCAGGTAAAG	4
EG7F2	CAPS	XbaI	GCATAGAATTTGACGATAACGAGC	GATCTGTGTAGGACTACGAGAC	5
CIW5	SSLP		GGTTAAAAATTAGGGTTACGA	AGATTTACGTGGAAGCAAT	4
NGA8	SSLP		TGGCTTTCGTTTATAAACATCC	GAGGGCAAATCTTTATTTCGG	4
T15L19SE	CAPS	AfaI	CAAGATTCAAACGGTTGAGGTGGG	CAAGACTATCATGCTGACATGTCG	4
CM4-3	CAPS	BglII	GATCAATAATAAGTGTCTTCTC	TTCTGGGTTCTTGGTGATCTC	4
MH8150	SSLP		CAGCAAGATTCTGCGGATTG	GACCAACAAGTGAGACCTGA	4
FCA11	CAPS	DraI	CGGTATCTCCAGGTGCGAGAC	GAGGACAAACATAACTACTGATAC	4
FCA2-190	CAPS	DdeI	TTCCTACACACTCACTACTCAG	TTCGTATATTGACTAGTGGATG	4
SC5	CAPS	AccI	CACAAGCTATACGATGCTCACC	TCGACGACTCTCAAGAACCC	4
G3883-1.4	CAPS	DdeI	TGTTTCAGAGTAGCCAATTC	CATCCATCAAACAAACTCC	4
CAT2	CAPS	DdeI	GACCAGTAAGAGATCCAGATACTGCG	CACAGTCATGCGACTCAAGACTTG	4
FCA38	CAPS	DraI	TTCCAGACTCGCATGTTGAG	TAACAATGGTAGAAACCATAAC	4
FCA312	CAPS	EcorI	ATCTCAAACCATCATTATCCAG	TCAAGAAAGACAATTCAGCTAC	4
M59	CAPS	BstuI	GTGCATGATATTGATGTACGC	GAATGACATGAACACTTACACC	1
MH6617	CAPS	PvuI	GGTAGAGAGCGTCCGGGACCTCG	TCAAATGTCGTAGTCAATGTCCGC	1
MH6715	CAPS	StyI	TGACCTAACGATCTTATCGTCTA	TCGTATGGCTTGTCTTCCATCTC	1
MH6810	CAPS	HhaI	AGGATCTCATTTCCCGACCAAAC	GGAGAATCTGCTTTCTTGCTGGT	1
CAT3	CAPS	HincII	CAGATGCAATGGCATCGTGGAG	CGGTGGTGCTCCAGTCTCCAAC	1
G2395	CAPS	XbaI	GGTTCCATCACCAAGCTCC	CTCCTTGTCTCCAGGTCCC	1
MH7400	CAPS	ApoI	GGATGAAGGCTTAGTACTGAATG	GCACTTTGTCAACATATGTAAGTT	1
M235	CAPS	HindIII	AGTCCACAACAATTGCAGCC	GAATCTGTTTCGCCTAACGC	1
PAI3	CAPS	MnlI	GACCCCTGCCAATGGGTGCAAGC	CACAGCTCTCTTTGAGGTAACTTC	1
G11447	CAPS	EcorV	CAGTGTGTATCAAAGCACCA	GTGACAGACTTGCTCCTACTG	1
ER	CAPS	DdeI	GAGTTTATTCTGTGCCAAGTCCCTG	CTAATGTAGTGATCTGCGAGGTAATC	2
RGA	CAPS	AfaI	TTCGATTCAGTTCGGTTTAG	GTTTAAGCAAGCGAGTATGC	2

Table 2. Steady state photosynthetic parameters of isolated mutants.

	Fv/Fm	1-qP	NPQ	Fv'/Fm'	ETR
WT	0.836±0.002	0.252±0.052	1.134±0.185	0.616±0.019	135.8±11.8
37-19-7	0.836±0.001	0.239±0.062	0.840±0.080	0.617±0.020	138.1±15.4
22-18-21	0.837±0.004	0.259±0.043	0.733±0.099	0.602±0.011	131.4±9.8
36-2-20	0.840±0.002	0.281±0.016	1.259±0.046	0.622±0.014	131.6±5.6
38-14-15	0.806±0.025	0.155±0.017	1.284±0.187	0.546±0.040	135.6±8.5

Photosynthetic parameters were measured at 700 μmol photons m^{-2} s^{-1} illumination. Prior to measurements, leaves are dark-adapted for at least 30 min. Data are expressed as the means of three individual leaves.

FIGURES

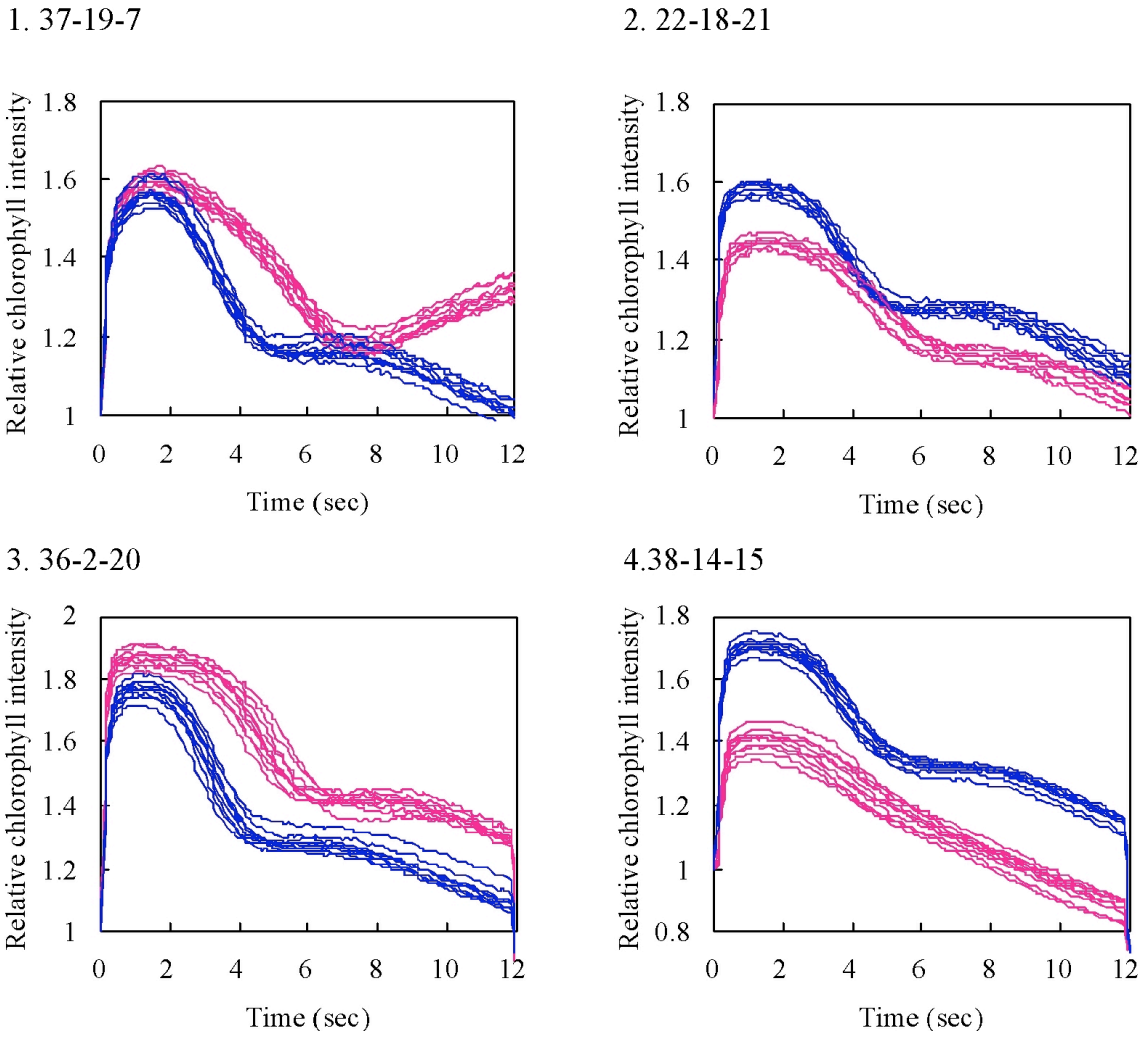

Figure 1. Time course changes of chlorophyll fluorescence intensity of isolated mutants. Chlorophyll fluorescence was monitored under illumination (350 µmol photons m^{-2} s^{-1}) for 12s. Pink and blue lines show isolated mutants and WT, respectively.

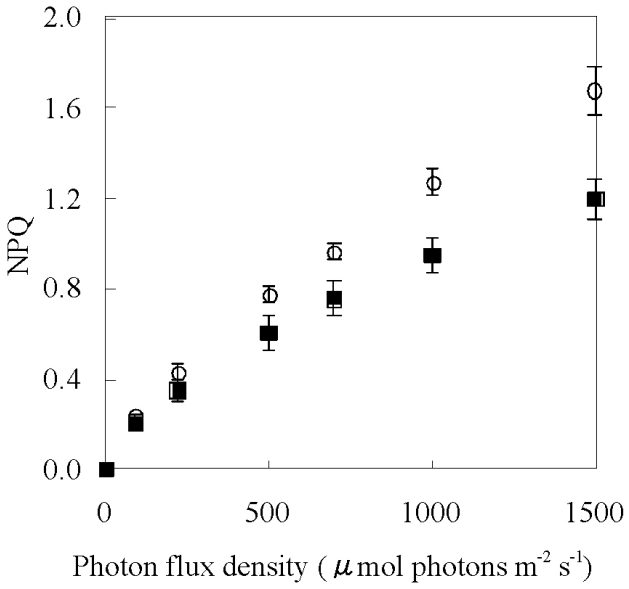

Figure 2. Photon flux density dependence of NPQ in the 37-19-7 mutant. Open circles and closed squares show NPQ of the WT and 37-19-7, respectively. Data are expressed as the means of three individual leaves.

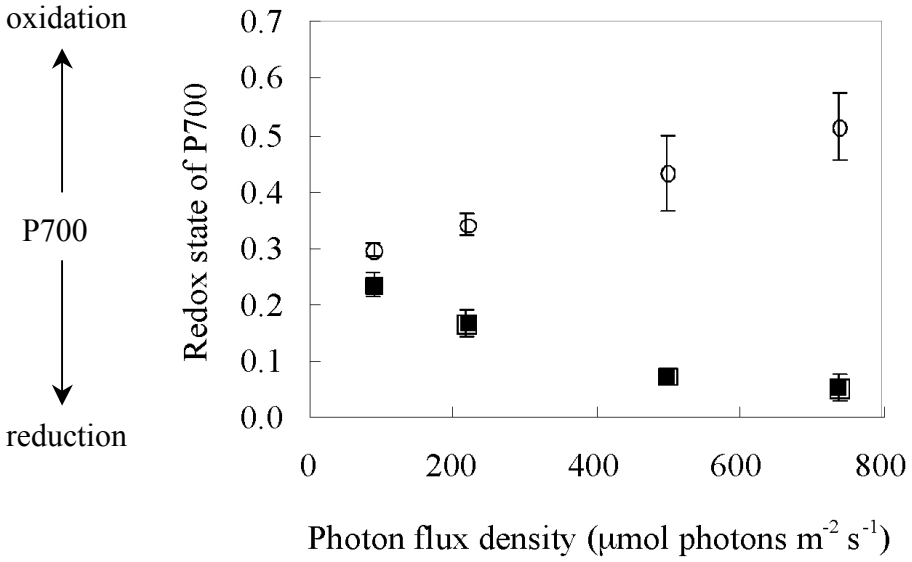

Figure 3. Steady-state level of the redox state of P700 in the 37-19-7 mutant. Open circles and closed squares show NPQ of the WT and 37-19-7, respectively. Dark-adapted leaves were illuminated at indicated photon flux densities. Data are expressed as the means of three individual leaves.

(A)

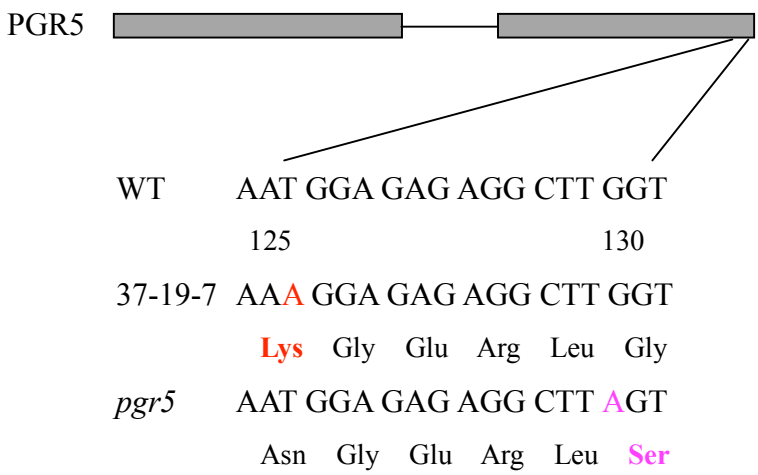

(B)

```
PGR5           1:MAAASISAIGCNQTLIGTSFYGGWGSSIS-GEDYQTMLSKTVAP------ 38
rice           1:MAAAAASSV--S--LPGARALPTWSSSVS-GDSHSLALSSWAAR------ 34
volvox         1:MLVAKRNAVQVRASGSAALSMSRSAAR-SVAVSSRIALSSWDDCRQTASS 49
Bassia         1:PT---------------------------------------------- 2
cyanobacteria  1:M----------------------------------------------- 1
Hyacinthus     1:RS---------------------------------------------- 2

PGR5          39:-----PQQARVSRKAIRAVPMMKNVNEGK-GLFAPLVVVTRNLVGKKRF  90
rice          35:-----PRSARPLRAPAR----MGNVNEGK-GIFAPVVVVVRNIVGRKRF  82
volvox        50:LAQS-APKLQNTSNAPRRKPVTMMGNKATTGPFAPLVVVVRGAIGEKEF  101
Bassia         3:----------------RAQPMMKNVNEGK-GIFA-VVVVTRNIIGKKRF  38
cyanobacteria  2:--------------------------------FAPIVILVRQQLGKAKF  22
Hyacinthus     3:----------------R--PMMGNVNEGK-GLFAPLVVVARNLVGKKTF  36
                                                 **  *   *   **  *

PGR5          91:NQLRGKAIALHSQVITEFCKSIGADAKQRQGLIRLAKKNGERLGFLA   133
rice          83:NQLRGKAIALHSQVITEFCKTIGADAKQRQGLIRLAKKNGEKLGFLA   125
volvox       102:NQFRGKAISLHSQVIKDFCKLLGVDNKQVQGVIRLAKKNGEKLGFLA   144
Bassia        39:NQLRGKAIALHSQVITEFCKSIGADAKQRQGLIRLAKKNGEKLGFLA    81
cyanobacteria 23:NQIRGKAIALHCQTITNFCNRVGIDAKQRQNLIRLAKSNGKTLGLLA    65
Hyacinthus    37:NQLRGKAIALHSQVINEFCKSIGADGKQRQGLIRLAKKNGEMLGFLA    79
                  ** ***** ** * *  **   * * ** *  ***** **  ** **
```

Figure 4. Map based cloning of the 37-19-7 mutant. (A) 37-19-7 and *pgr5* mutantion in the *pgr5* gene. Gray boxes show exons and thin lines show introns. (B) Alignment of amino acid sequences in PGR5 homologs. Astarisks indicate conserved amino acids between PGR5 and PGR5 homologs from rice, volvox, bassia, cyanobacteria and hyacinthus. Red and pink characters indicate the 37-19-7 and *pgr5* mutation, respectively.

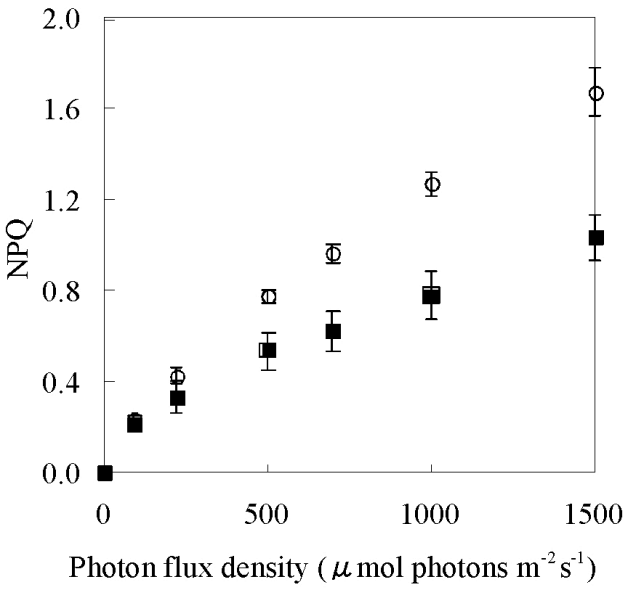

Figure 5. Photon flux density dependence of NPQ in the 22-18-21 mutant. Open circles and closed squares show NPQ of WT and 22-18-21, respectively. Data are expressed as the means of three individual leaves.

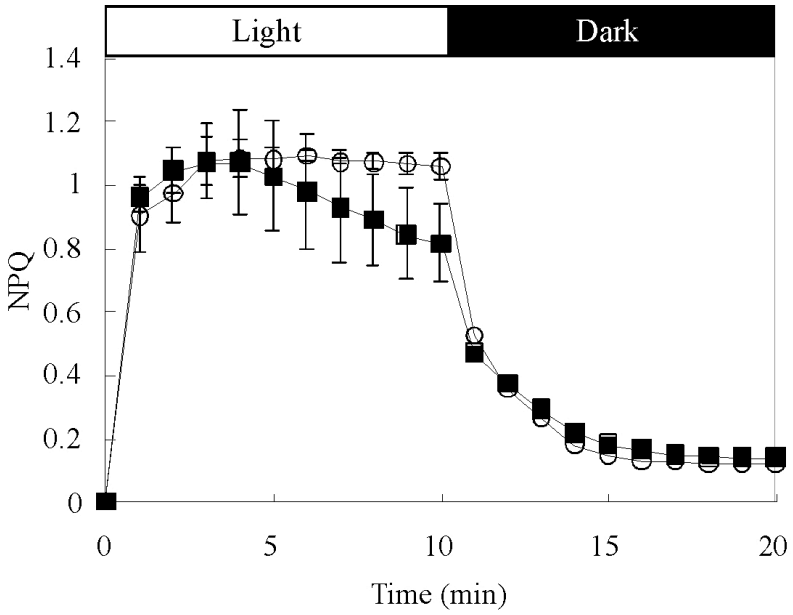

Figure 6. Time course of NPQ induction in the 22-18-21 mutant. NPQ was measured at 700 μmol photons m^{-2} s^{-1} illumination. Open circles and closed squares show NPQ of WT and 22-18-21, respectively. Data are expressed as the means of three individual leaves. Prior to measurements, leaves are dark-adapted for at least 30 min.

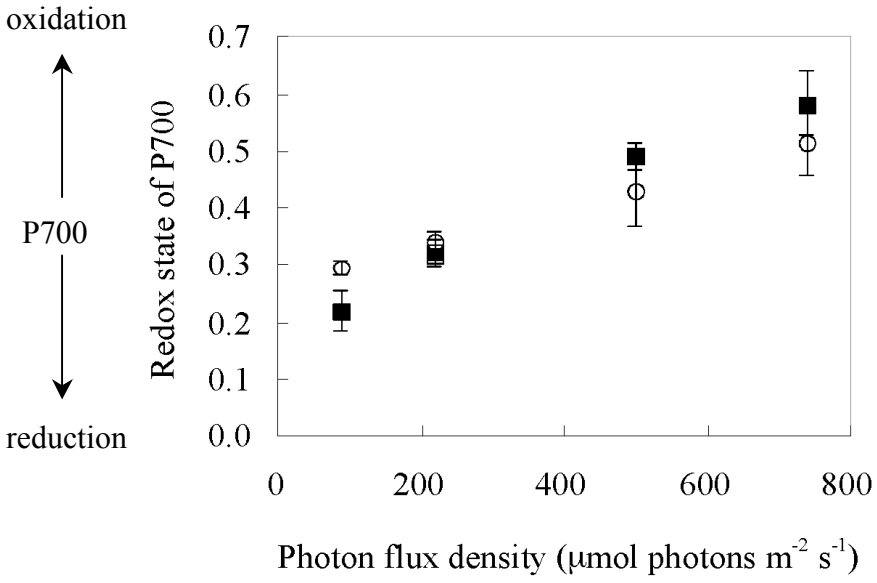

Figure 7. Steady-state level of the redox state of P700 in the 22-18-21 mutant. Open circles and closed squares show NPQ of the WT and 22-18-21, respectively. Dark-adapted leaves were illuminated at indicated photon flux densities. Data are expressed as the means of three individual leaves.

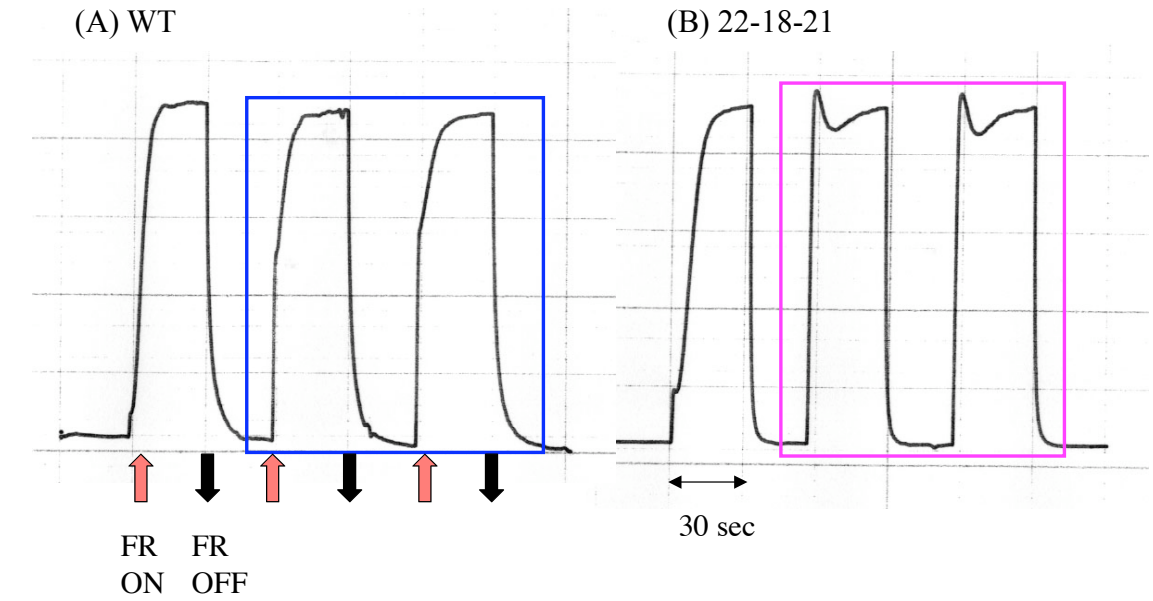

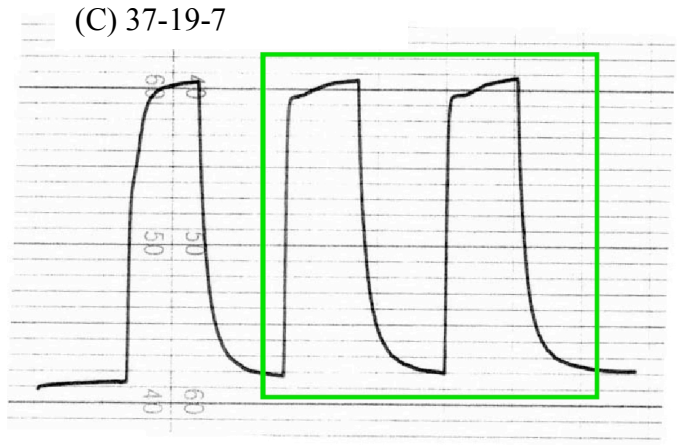

Figure 8. The oxidation kinetics of P700 by far-red light. Detached leaves were illuminated with far-red light (30 sec) for three times. Prior to measurements, leaves are dark-adapted for at least 30 min.

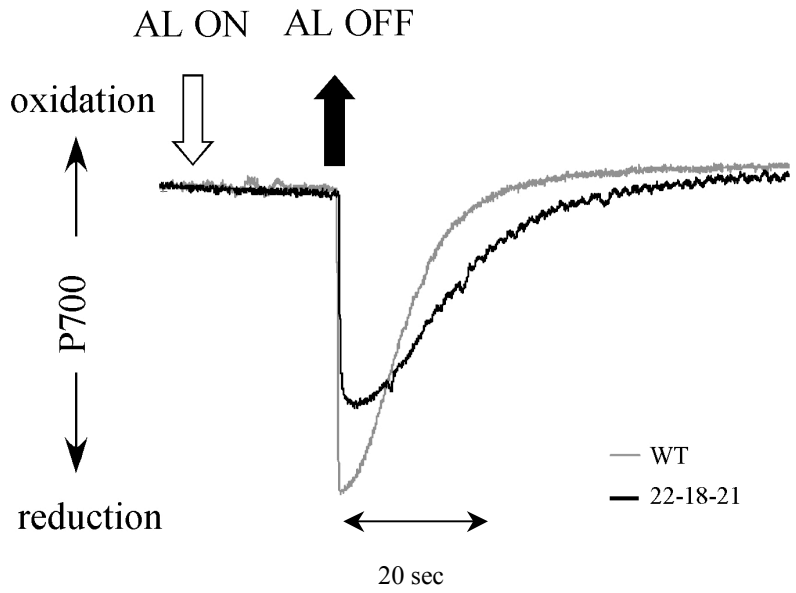

Figure 9. The kinetics of changes in redox state of P700 in the 22-18-21 mutant. The redox kinetics of P700 was monitored after termination of actinic light illumination (700 μmol photons m^{-2} s^{-1}) under a background of far-red. Dark-adapted leaves were illuminated with background far-red light for 2min before actinic light off. Gray and black lines show WT and 22-18-21, respectively.

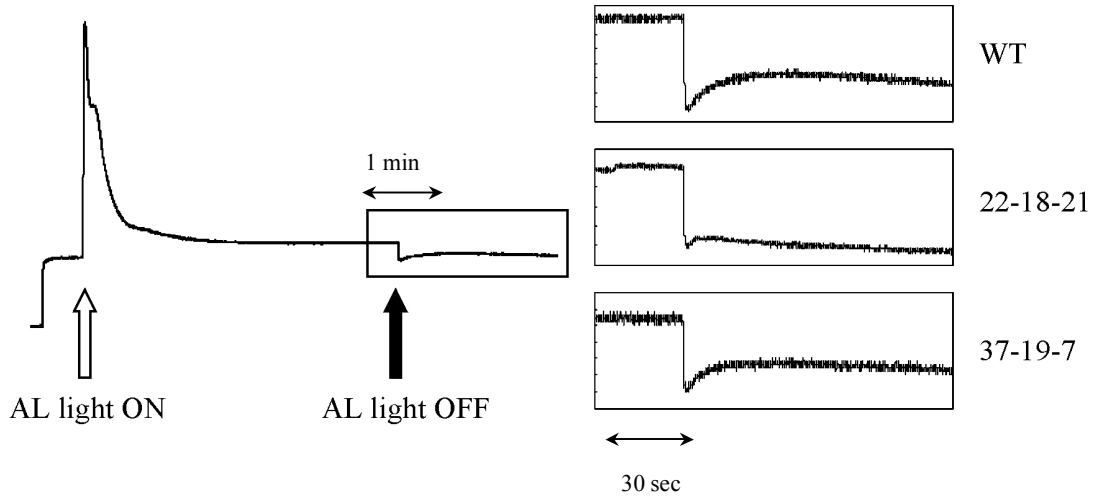

Figure 10. The transient increase of chlorophyll fluorescence in the dark. (A) The trace of chlorophyll fluorescence intensity in WT. Dark-adapted leaf was illuminated (200 μmol photons m^{-2} s^{-1}) for 2 min. (B) A boxed region of (A) is closed up in WT (upper), 22-18-21 (middle) and 37-19-7 (lower).

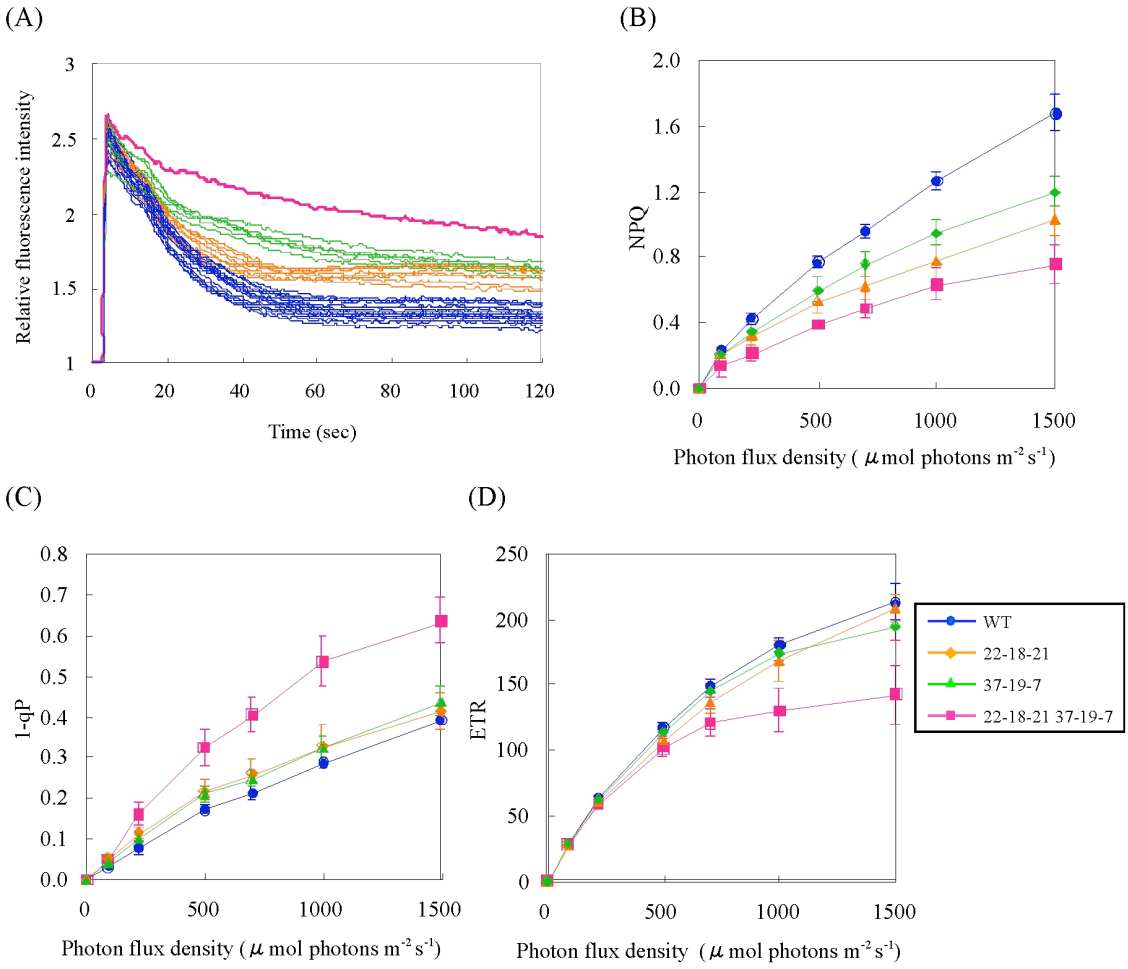

Figure 11. Chlorophyll fluorescence analysis of single and double mutants (A) The chlorophyll fluorescence kinetics of F2 populations crossed between 22-18-21 and 37-19-7. Chlorophyll fluorescence kinetics was monitored using chlorophyll fluorescence imaging system. Photon flux density dependence of NPQ (B), 1-qP (C) and ETR (C). Data are expressed as the means of three individual leaves.

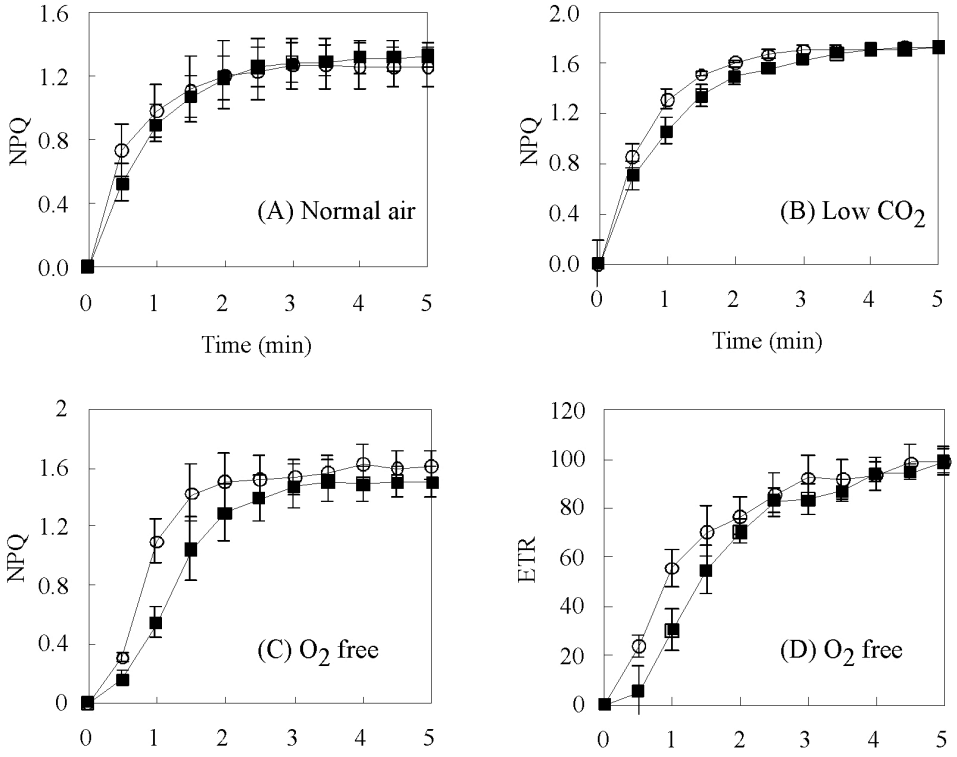

Figure 12. Time course of NPQ induction under various air conditions. Induction of NPQ and ETR was monitored in the air (A), low CO_2 (0.003%) (B) or N_2 gas with 0.03% CO_2 (C, D) conditions. Photon flux density of actinic light is 700 (A, C, D) or 200 (B) μmol photons m^{-2} s^{-1}. Open squares and close circles represent NPQ of WT and *hma1*, respectively. Data are expressed as the means of at least three measurements of different leaves. Prior to measurements, leaves are dark-adapted for at least 30 min.

(A)

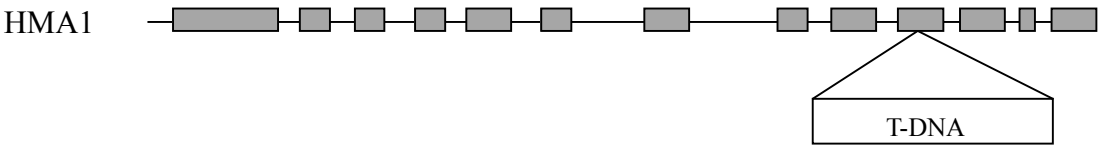

(B)

chloroplast transit peptide

```
MEPATLTRSSSLTRFPYRRGLSTLRLARVNSFSILPPKTLLRQKPLRISASLNLPPRSIR 60

                    poly-His
LRAVEDHHHDHHHDDEQDHHNHHHHHHQHGCCSVELKAESKPQKMLFGFAKAIGWVRLAN 120

YLREHLHLCCSAAAMFLAAAVCPYLAPEPYIKSLQNAFMIVGFPLVGVSASLDALMDIAG 180

GKVNIHVLMALAAFASVFMGNALEGGLLLAMFNLAHIAEEFFTSRSMVDVKELKESNPDS 240

ALLIEVHNGNVPNISDLSYKSVPVHSVEVGSYVLVGTGEIVPVDCEVYQGSATITIEHLT 300

GEVKPLEAKAGDRVPGGARNLDGRMIVKATKAWNDSTLNKIVQLTEEAHSNKPKLQRWLD 360

EFGENYSKVVVVLSLAIAFLGPFLFKWPFLSTAACRGSVYRALGLMVAASPCALAVAPLA 420

YATAISSCARKGILLKGAQVLDALASCHTIAFDKTGTLTTGGLTCKAIEPIYGHQGGTNS 480

SVITCCIPNCEKEALAVAAAMEKGTTHPIGRAVVDHSVGKDLPSIFVESFEYFPGRGLTA 540

TVNGVKTVAEESRLRKASLGSIEFITSLFKSEDESKQIKDAVNASSYGKDFVHAALSVDQ 600

KVTLIHLEDQPRPGVSGVIAELKSWARLRVMMLTGDHDSSAWRVANAVGITEVYCNLKPE 660

DKLNHVKNIAREAGGGLIMVGEGINDAPALAAATVGIVLAQRASATAIAVADILLLRDNI 720

TGVPFCVAKSRQTTSLVKQNVALALTSIFLAALPSVLGFVPLWLTVLLHEGGTLLVCLNS 780

VRGLNDPSWSWKQDIVHLINKLRSQEPTSSSSNSLSSAH                     819
```

Figure 13. PCR-based cloning of the 36-2-20 mutant. (A) Position of T-DNA in *hma1* gene. Gray boxes show exons and thin lines show introns. (B) Deduced amino acid sequences of HMA1. Dashed lines show transmembrane domain. Box in the 6th transmembrane domain shows Ser-Pro-Cys motif. The N-terminal end has a poly-His domain.

(A) Control

(B) 100 μM $ZnSO_4$

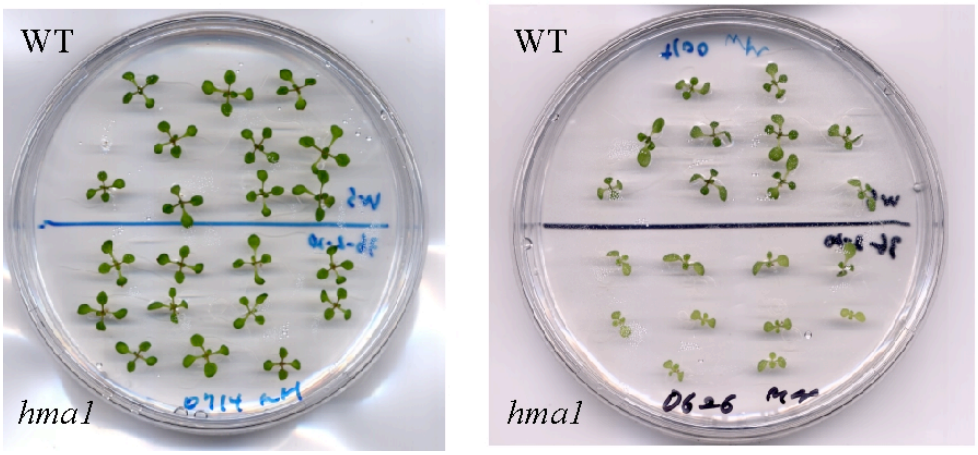

Figure 14. Zn sensitivity of *hma1*. Plants were grown in MS agar medium with 1% (w/v) sucrose in the absence (A) or in the presence of 100 μM $ZnSO_4$ (B). WT and *hma1* are grown in upper and lower half of the plates, respectively.

(A)

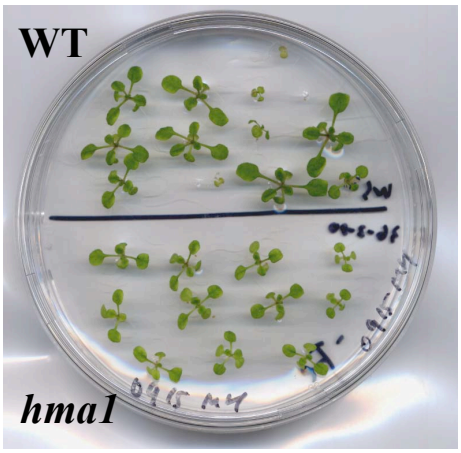

(B)

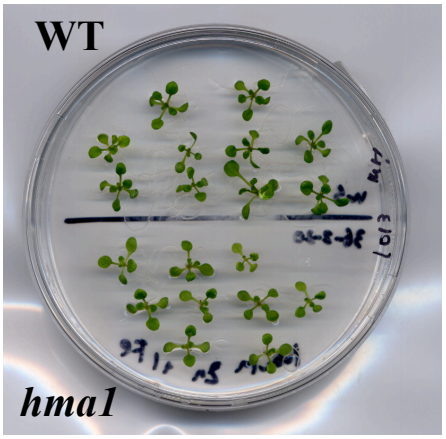

(C)

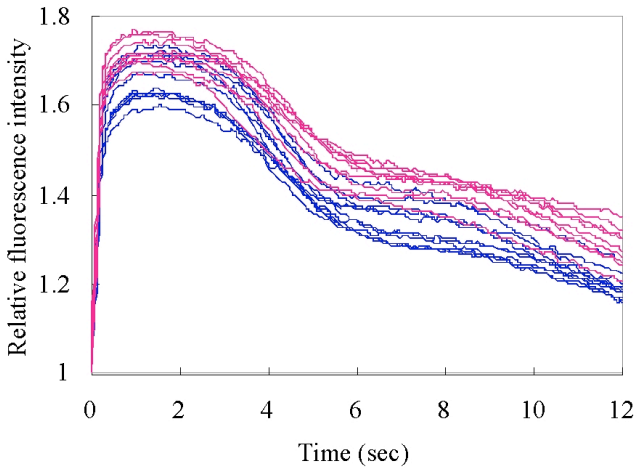

Figure 15. The effect of Fe in *hma1*. Plants were grown in MS agar medium with 1% (w/v) sucrose in the absence of $FeSO_4$ (A) and in the presence of 100 μM $ZnSO_4$ supplemented with 150 μM $FeSO_4$ (B). WT and *hma1* are grown in upper and lower half of the plates, respectively. (C) Chlorophyll fluorescence analysis. Chlorophyll fluorescence kinetics was monitored in the MS medium supplemented with 250 μM Fe SO_4. Blue and pink lines show WT and *hma1*, respectively.

(A) WT

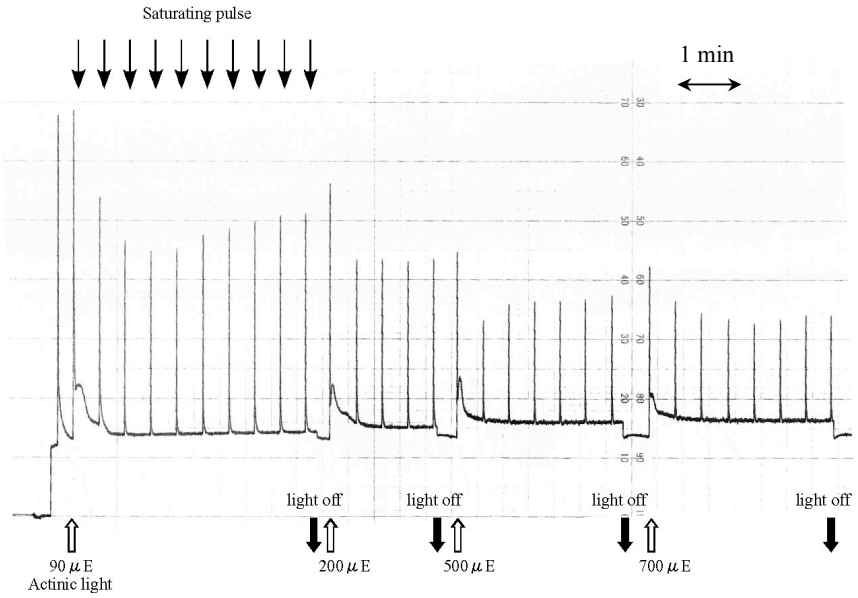

(B) 38-14-15

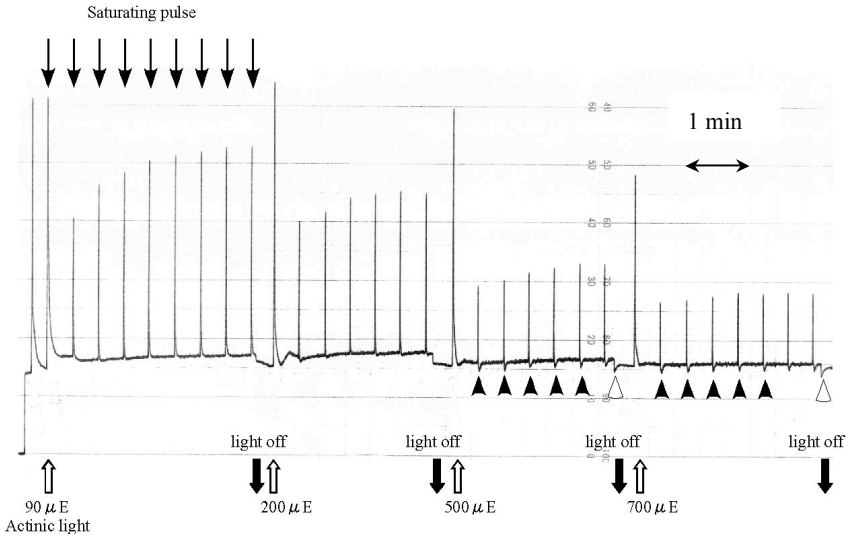

Figure 16. Chlorophyll fluorescence kinetics by PAM fluorometer. Chlorophyll fluorescence intensity was monitored in WT (A) and 38-14-15 mutant (B). Closed arrows, actinic light off. Open arrows, actinic light on. Leaves were dark-adapted for at least 30 min prior to measurements.

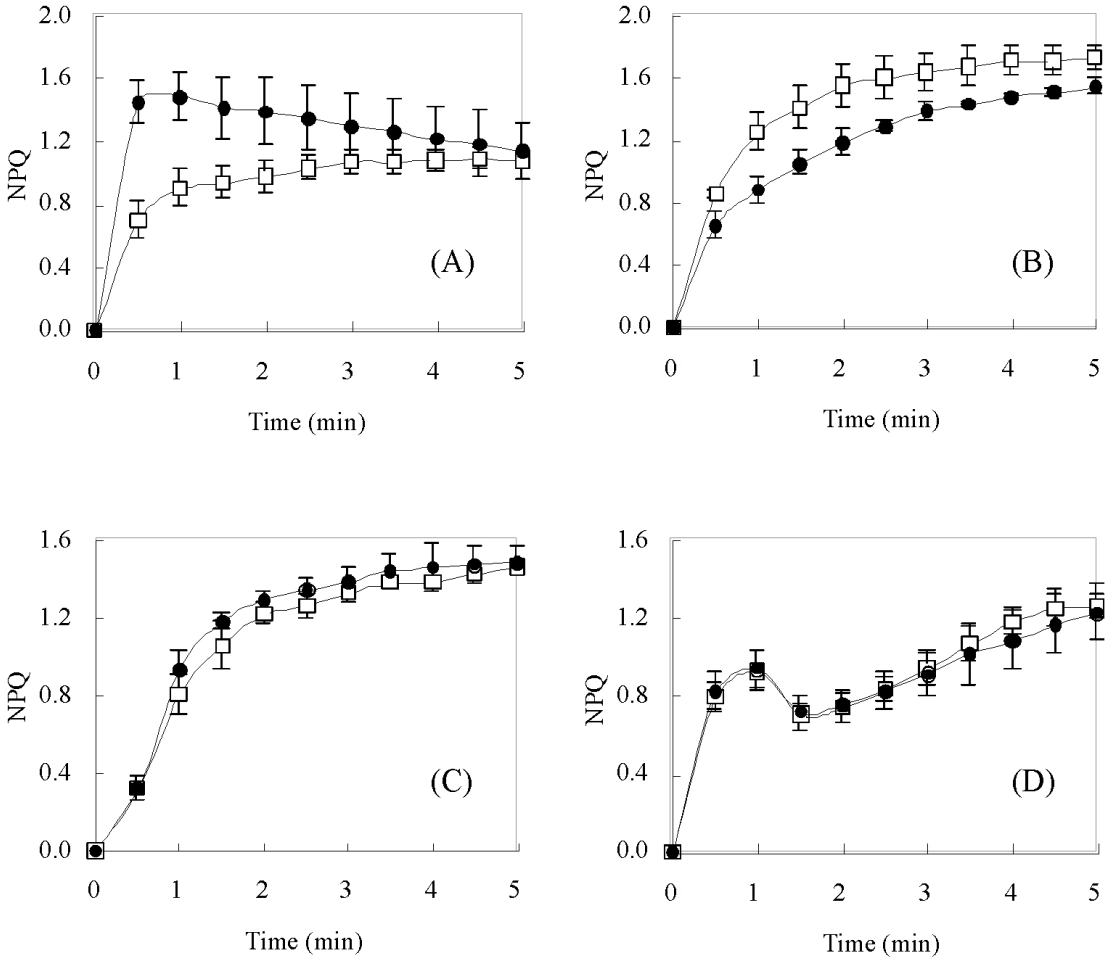

Figure 17. Alternative electron transport activity in the 38-14-15 mutant. Induction of NPQ was monitored in the air (A), low CO_2 (0.003%) (B), N_2 gas with 0.03% CO_2 (C) or high CO_2 (0.2%) conditions (D). Photon flux density of actinic light is 700 (A, C, D) or 200 (B) □mol photons m^{-2} s^{-1}. Open squares and close circles represent WT and 38-14-15, respectively. Data are expressed as the means of at least three measurements of different leaves.

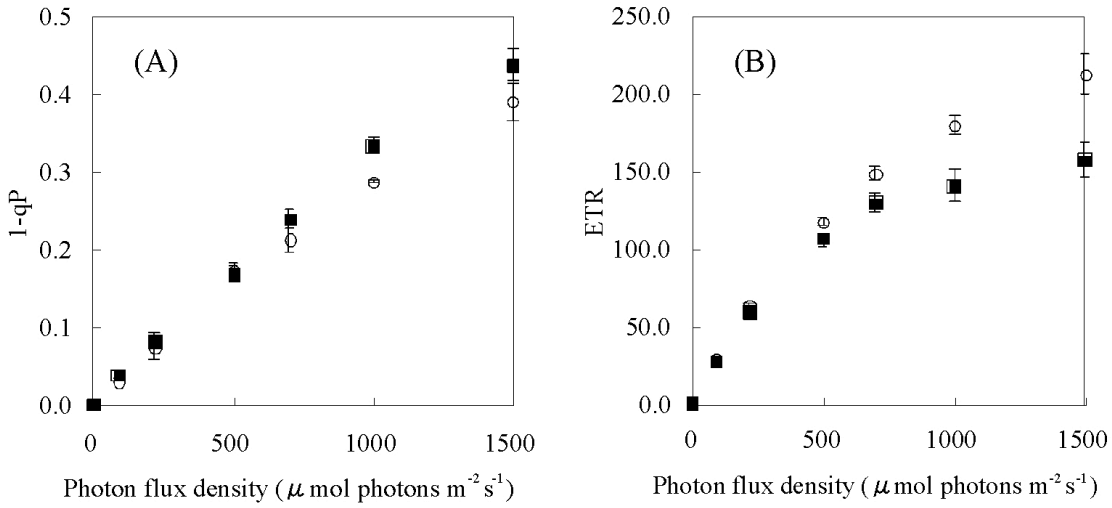

Figure 18. Photon flux density dependence of 1-qP and ETR in the 38-14-15 mutant. Open circle and closed square show 1-qP (A) and ETR (B) of the WT and 38-14-15, respectively. Data are expressed as the means of three individual leaves.

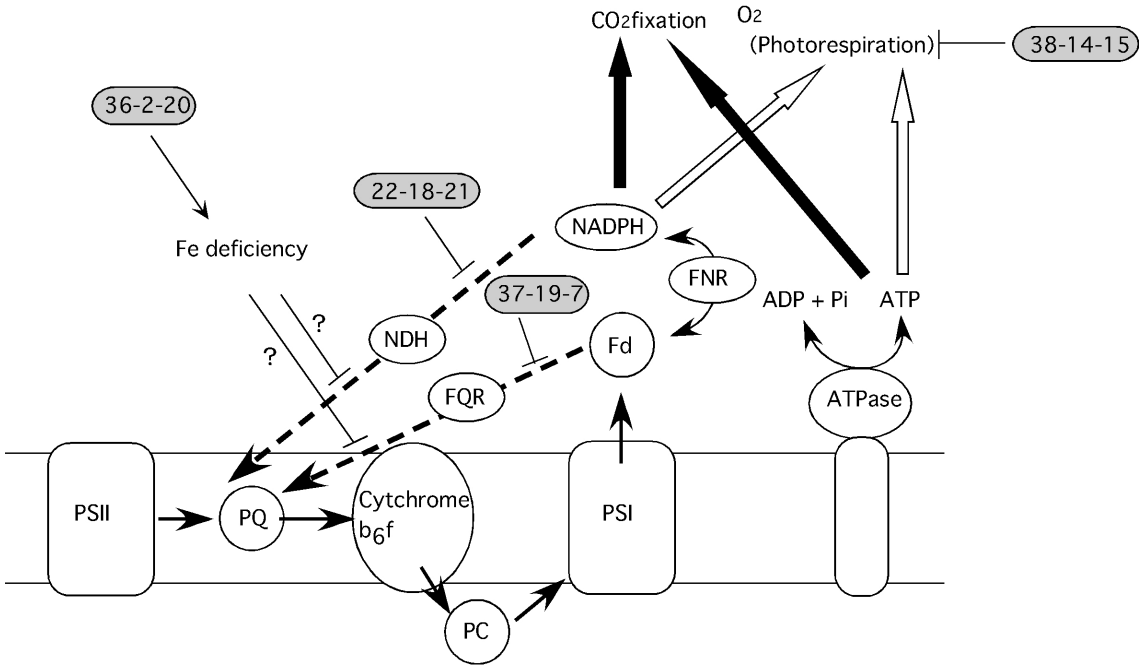

Figure 19. The summarized scheme of defects in isolated mutants. Thick solid lines show linear electron transport pathway. Gray boxes show isolated mutants in this study. Dashed lines and open arrows show cyclic electron flow around PSI and photorespiration pathway, respectively.